CHAPTER

8

Basic Josephson Junctions

8.1 INTRODUCTION

The macroscopic quantum model that was introduced in Chapter 5 provided a framework for understanding the basic electrodynamics of superconductors. This model assumes that the superelectrons can be described by a macroscopic wavefunction $\Psi(\mathbf{r},t)$ that satisfies the Schrödingerlike equation and whose squared modulus is the density of superelectrons, $n^*(\mathbf{r},t)$. In Section 5.4 we further assumed that the wavefunction is of the form $\Psi(\mathbf{r},t) = \sqrt{n^*} \exp i\theta(\mathbf{r},t)$, which led to the following for an isotropic superconductor with a constant n^* :

$$\mathbf{J}_{s}(\mathbf{r},t) = -\frac{1}{\Lambda} \left[\mathbf{A}(\mathbf{r},t) + \frac{\Phi_{o}}{2\pi} \nabla \theta(\mathbf{r},t) \right]$$
 (8.1)

and

$$\frac{\partial}{\partial t} \theta(\mathbf{r}, t) = -\frac{1}{\hbar} \left[\frac{\Lambda \mathbf{J}_{s}^{2}}{2n^{\star}} + q^{\star} \phi(\mathbf{r}, t) \right] . \tag{8.2}$$

Equation 8.1 is the supercurrent equation (introduced in Equation 5.81) and describes the current density of the superelectrons in a single piece of material. Equation 8.2 is the energy-phase relationship (introduced in Equation 5.84) and shows how the phase of the wavefunction changed in time with the energy of the superelectrons. The London coefficient Λ (Equation 2.132) is related to the penetration depth by

$$\Lambda = \mu_o \lambda^2 = \frac{m^*}{n^* (q^*)^2}. \tag{8.3}$$

We also found in Chapter 5 that the time derivative of Equation 8.1 led to a description of perfect conductivity through the first London equation; the curl of Equation 8.1 to perfect diamagnetism through the second London equation; and the line integral to fluxoid quantization. In all these cases the supercurrent has been driven by electric and magnetic fields. In this chapter we show that a

supercurrent can be induced by maintaining a difference in the phase θ through a process known as *tunneling*. When this phase is maintained between two separated superconductors, a supercurrent results and is known as the Josephson effect.

The concept of tunneling is a direct consequence of quantum mechanics. One of the fundamental ideas of quantum mechanics is the wave-particle duality of nature. We have already seen this idea in Chapter 5 where entities that we classically think of as wave phenomena can be just as readily considered as particles. The reverse is also true; although classically we think of an electron as a particle, it is just as appropriate to describe it in terms of a wave phenomenon. The consequences of these "matter waves" are far reaching. Just as stray fields leak out of electromagnetic structures, so too, matter can "leak out" of a confinement. Perhaps the best-known example of this is the radioactive decay of an atomic nucleus. Although the protons and neutrons are tightly bound in the nucleus, it is possible for them to tunnel out of the nucleus by this quantum mechanical mechanism.

Electrons can be observed to tunnel as well. Suppose we take a piece of metal, coat its surface with a very thin layer of insulating material, and then place another piece of metal on top of that. The geometry of such a sandwich structure, known as a tunnel junction, is shown in Figure 8.1. If we try to drive a dc current through the junction, classically we would expect it would be impossible; the electrons would not be able to pass through the insulating layer. Indeed, the junction resembles a simple capacitor (with very thick plates!) and the impedance of a capacitor at zero frequency is infinite. From quantum mechanics, however, we know that the electrons' matter waves can stray across the barrier. There is a very small, but nonzero, probability therefore for an electron to tunnel through the insulating region. We can increase the probability

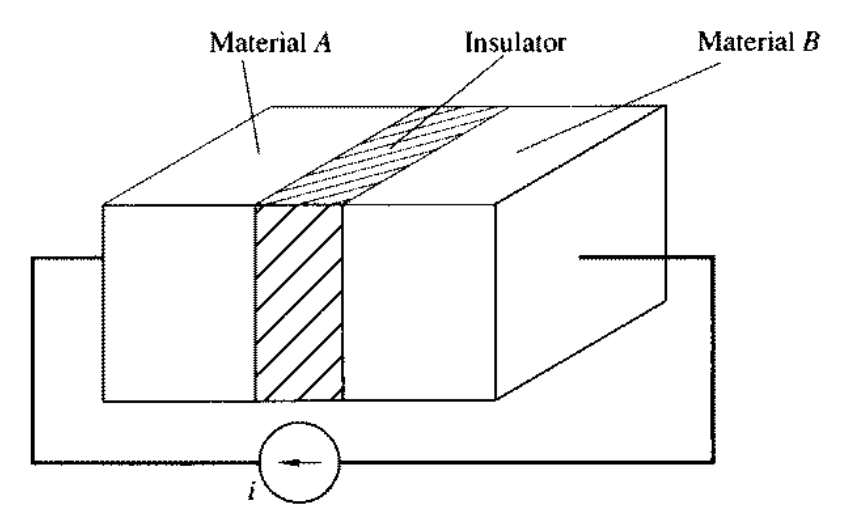


Figure 8.1 A tunnel junction. Materials *A* and *B* can be either a normal metal or a superconductor. The insulating region is greatly exaggerated in size for clarity and is very thin in reality.

8.1 Introduction 395

of having an electron pass through the barrier by making the insulator very thin (say 10 Å thick) and having many carriers available for tunneling (as is in a metal). Under these conditions, it is possible to pass an observable dc current through the structure.

Ivar Giaever used these ideas to explain an interesting series of experiments he performed in 1960. Giaever was interested in observing electron tunneling between a normal metal and a superconductor. He therefore fabricated lead-(aluminum oxide)-aluminum junctions. The classification of such tunnel junctions is known as SIN junctions; the acronym standing for superconductor-insulator-normal metal. (The aluminum is the normal metal in this case since the junction is maintained at a temperature below the critical temperature for the lead, but above the critical temperature for aluminum.) Giaever found that when the junction was cooled below T_c , the resistance of the structure (given by the inverse slope of the i-v characteristic) increased for a range of voltages as shown in Figure 8.2. This result may at first seem paradoxical, but in fact, Giaever realized that this effect is very well explained in terms of the gap predicted by the BCS theory.

Recall from Section 1.3 that the superelectrons can be envisioned as bound in pairs and that the binding energy is given by 2Δ . Suppose a Cooper pair is split up, in the sense that the electrons are no longer part of the superelectron fluid. Each electron would therefore have an energy of at least Δ — otherwise they would pair again (though not necessarily with each other). In other words, the normal electrons in a superconductor all have an energy at least Δ above the energy they would have if the material were not superconducting.

We know that when we pass a dc current through an SIN junction, the carriers must be normal electrons since Cooper pairs do not exist in the normal metal. We just observed, however, that all normal electrons in a superconductor

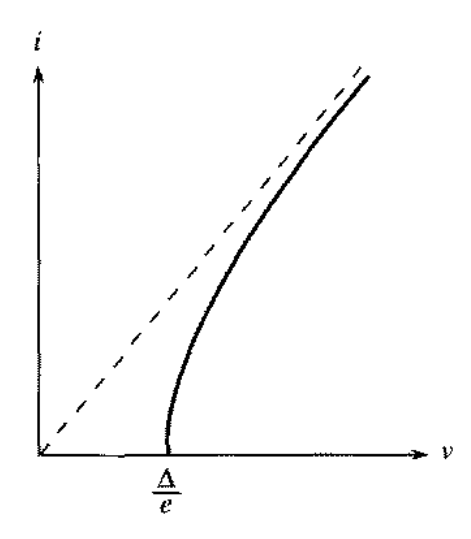


Figure 8.2 An idealized form of the i-v curve for an NIS tunnel junction. The solid line is the characteristic for temperatures below T_c , the dotted line for temperatures above T_c .

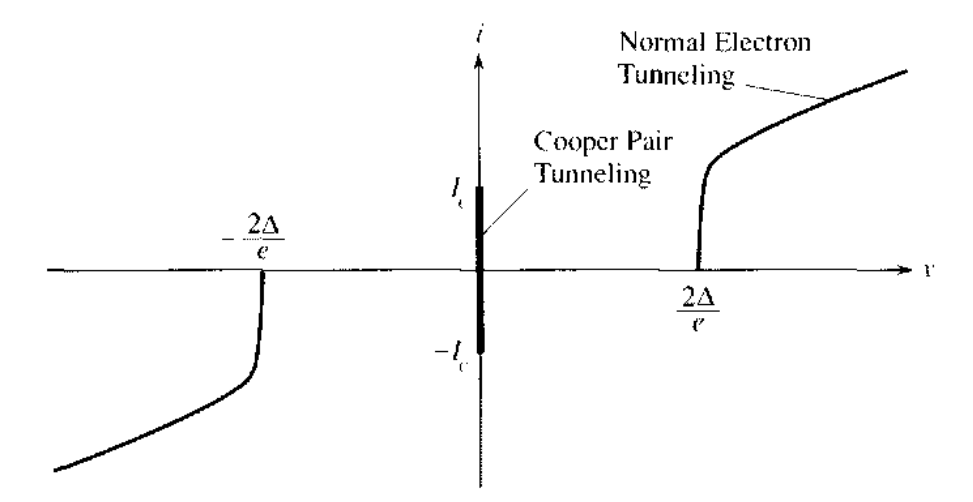


Figure 8.3 The i-v curve for a Josephson junction. The Josephson current is represented by the current at zero voltage.

are elevated in energy by an amount Δ . The only conclusion then is that for a normal electron to tunnel from the metal into the superconductor we must increase its energy by an amount Δ . We therefore cannot expect to pass any current until the junction is biased by a voltage of at least Δ/e , where e is the charge on an electron. This is precisely what we observe in Figure 8.2.

Suppose we now consider the case of superconductor-insulator-superconductor (SIS) tunneling between two identical superconductors. Now there are no normal electrons available as with the metal in the previous case. We must therefore break Cooper pairs so that the electrons can tunnel across the insulating region and carry current. As a result, we expect to see a similar i-v characteristic, only now the minimum voltage necessary to produce a current is $2\Delta/e$, and indeed this is observed.

What about a *Cooper pair* tunneling through the barrier? The general consensus among researchers before 1962 was that such an event would not happen often enough to be statistically significant. The reasoning was that as the tunneling of an electron has a very small chance of occurring, the tunneling of both electrons in a Cooper pair simultaneously crossing the insulator would be astronomically small. In 1962, however, Brian Josephson changed the popular wisdom.

From his calculations using the BCS theory, Josephson discovered that the probability of a Cooper pair tunneling through the barrier was the *same* as that for a single electron. The reason is that the tunneling for a Cooper pair is an ordered, coherent process. In other words, we should not imagine the situation to be two electrons' matter waves leaking across the insulating barrier. Instead, it is the macroscopic wave function that tunnels from one superconductor to the other. By 1963 Philip Anderson and John Rowell had experimentally confirmed the existence of Cooper pair tunneling.

The i-v curve for an SIS or *Josephson junction* is shown in Figure 8.3. As expected we have branches similar to those in the i-v characteristic of an

8.1 Introduction 397

SIN junction and these branches represent the normal electron tunneling. The current at zero voltage is a direct result of the Cooper pair tunneling and is known as the *Josephson current*. The curve at zero voltage represents the range of currents that can flow by Josephson tunneling. These currents require *no* voltage for them to pass through the insulating region and their behavior is fundamentally important to many practical applications that we now survey.

Because of Josephson tunneling, we can apply a dc current to the junction and not develop a voltage drop across it. However, there is a limit to the amount of current that the tunneling Cooper pairs can carry and so if too much current is applied, the Josephson effect is lost and the current is carried by the normal electrons. The maximum dc current density that can be passed through the junction at zero voltage is known as the *Josephson critical current density* J_c . When the applied current exceeds the critical current density, of course, we will develop a voltage drop across the junction. In other words, we have switched from a zero voltage to a finite voltage state by increasing the dc current, allowing us to develop a binary digital logic.

Let us compare this form of digital technology to that based on semiconductors. The first thing to notice is that when a Josephson junction switches, the voltage across it is typically on the order of millivolts for conventional superconductors. Semiconductor logic, on the other hand, requires a potential on the order of volts to switch binary states. Thus the Josephson junction made of conventional superconductors requires three orders of magnitude less power to operate than standard semiconductor logic, making such a system more energy efficient. Moreover, the superconducting logic generates less heat and, as a result, can be packed more densely than the semiconducting equivalent.

Thus far, we have examined what happens when we apply a dc current to a Josephson junction. What happens if we were to apply a dc voltage? If the applied voltage exceeds the energy required to break Cooper pairs, we will return to the situation where the normal electrons tunnel and carry current. Suppose, however, that our applied voltage was less than the threshold, $2\Delta/e$. Such a voltage increases the energy of a Cooper pair and, surprisingly, the Cooper pairs respond by oscillating back and forth across the junction. In some cases, the junction will radiate an electromagnetic field. Because the frequency of oscillation is related to the applied voltage, we could now use this junction to create a precision oscillator. Conversely, by subjecting the junction to a time varying electromagnetic field, we can induce a voltage across it. Since it is relatively easy to measure frequencies to high precision, we can use the Josephson junction as a robust voltage standard. Indeed, this is currently the method with which many countries determine the voltage standard.

Just as the behavior of a superconductor is sensitive to a magnetic field, so too is a Josephson junction. In fact, the maximum Josephson current possible is modulated by the magnetic field in which a junction is placed. Because Josephson tunneling is another macroscopic manifestation of the inherently quantum mechanical behavior of superconductors, it is effected by even the smallest amount of flux. Josephson junctions have been successfully used

in magnetometers known as SQUIDs (superconducting quantum interference devices) that are sensitive to fluxes as small as a fraction of Φ_o . Thus, we discover that the many consequences of the coherent tunneling can be used in a number of practical ways.

In this chapter we are only concerned with describing the Josephson current that occurs at zero voltage and that can be described by the macroscopic wavefunction. In fact, under our development, it is the normal electrons' tunneling that is more difficult to describe. The discussion of this topic will be given in Chapter 9.

In Section 8.2 we first consider tunnel junctions and find a relationship between the supercurrent density and the difference in phase of the wavefunction across the junction. We find that the supercurrent density through the tunnel junction varies sinusoidally with the difference in phase across the junction and has a maximum value known as the critical current density J_c . Throughout this chapter we consider current densities that are always less than J_c so that the current is always a supercurrent; we refer to such junctions as basic Josephson junctions. In Chapter 9 we consider the situation in which the current density can exceed J_c , and refer to that junction as a generalized Josephson junction.

In Section 8.3 we restrict ourselves to the cases where the junction area is small enough so that the junction can be represented as a lumped circuit element. The current rather than the current density is sufficient to describe such a basic lumped Josephson junction. We discuss the energy stored in such lumped basic Josephson junctions and the dynamics of some simplified circuits. In Section 8.4 we show how a circuit with two basic lumped Josephson junctions can be configured to make a superconducting quantum interference device, known as a SQUID, which is a very sensitive detector of magnetic fields. In Sections 8.5 and 8.6 we relax the restrictions on the junction area so that the junctions are distributed systems where the currents can have a spatial dependence inside the junction itself.

8.2 JOSEPHSON TUNNELING

Consider the tunnel junction in Figure 8.4, which shows a current source driving a current from the superconductor in region 1 across an insulating barrier of thickness 2a into the superconductor in region 2. In general, the supercurrent density $J_s(x,y,z,t)$ in each superconductor is given by the supercurrent equation of Equation 8.1. The supercurrent density at the edges of the junction at $x = \pm a$ is denoted by $J_o(\pm a, y, z, t)$. We would like to find a relationship between the current density at the insulating boundaries and the value of the phase of the wavefunction at each boundary. To do so, two simplifying assumptions are made. The first is to consider the junction area (wd) to be small enough so that the current density can be considered uniform. (The length scale over which this approximation is valid is discussed in Sections 8.5 and 8.6.) We denote this uniform current density by J_o . The second assumption is to consider

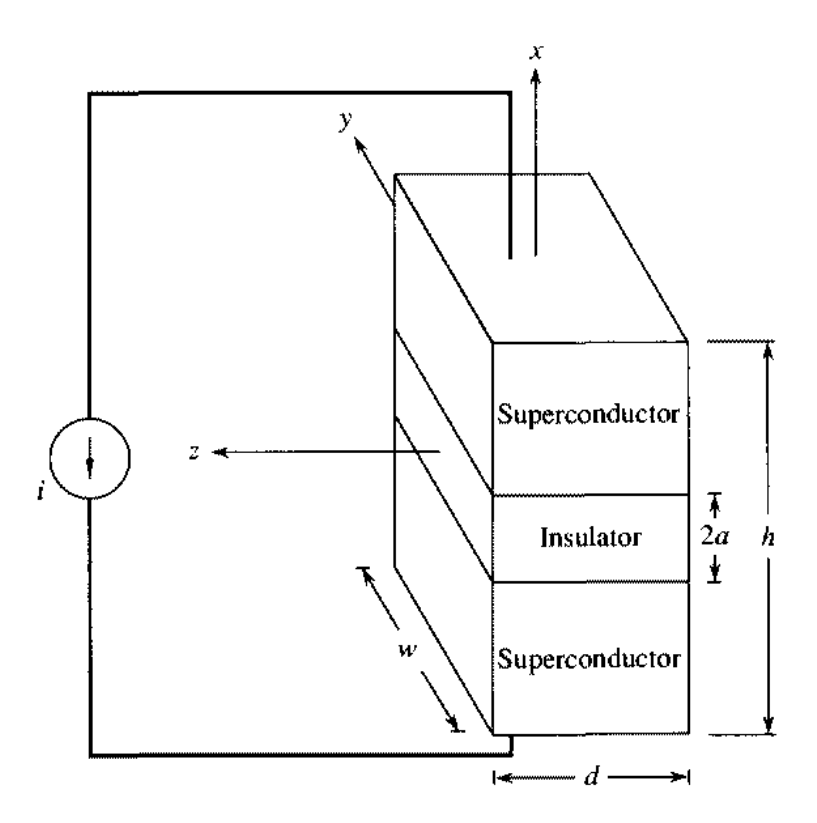


Figure 8.4 A Current Source Driving a Current across a Tunnel Junction

the magnetic vector potential to be zero, as it would be in the absence of any electric and magnetic fields. After finding the relationship between the current density and the phase at the insulating boundaries, we relax these two simplifying assumptions. Consequently, the supercurrent density in the superconductors at the superconductor-insulator boundaries $x = \pm a$ is given by Equation 8.1 as

$$\mathbf{J}_{\mathrm{s}}(\pm a,t) = -\frac{\Phi_{o}}{2\pi\Lambda}\nabla\theta(\pm a,t) = \mathbf{J}_{\mathrm{o}}.$$
 (8.4)

Likewise, in the absence of electric and magnetic fields, Equation 8.2 yields

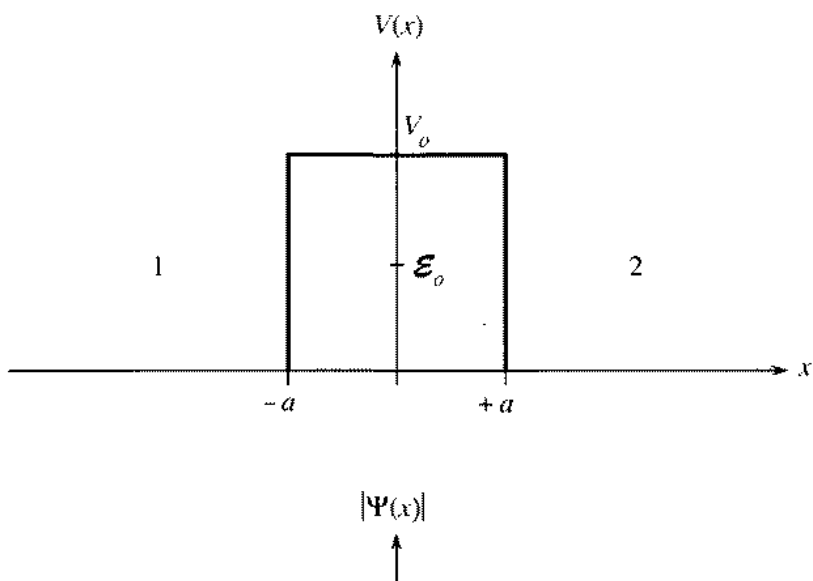
$$\frac{\partial}{\partial t}\theta(\pm a,t) = -\frac{1}{\hbar}\left(\frac{\Lambda J_o^2}{2n^*}\right) = -\frac{\mathcal{E}_o}{\hbar}, \qquad (8.5)$$

where $\mathcal{E}_o = m^* v_s^2 / 2$ is the kinetic energy due to the moving superelectrons and is a constant. Consequently, the time dependent wavefunction can be written as

$$\Psi(\mathbf{r},t) = \Psi(\mathbf{r}) e^{-i(\mathcal{E}_o t/\hbar)}, \qquad (8.6)$$

where $\Psi(\mathbf{r})$ is the time independent wavefunction.

We must now find the wave equation for the superconducting pairs when they are in the insulator. We model the insulator as a region with a constant potential V_o that is greater than \mathcal{E}_o . Figure 8.5 shows how the potential V(x) is modeled across the junction. With classical equations of motion from Newton's laws, the superelectron in region 1 would have to maintain the same energy \mathcal{E}_o



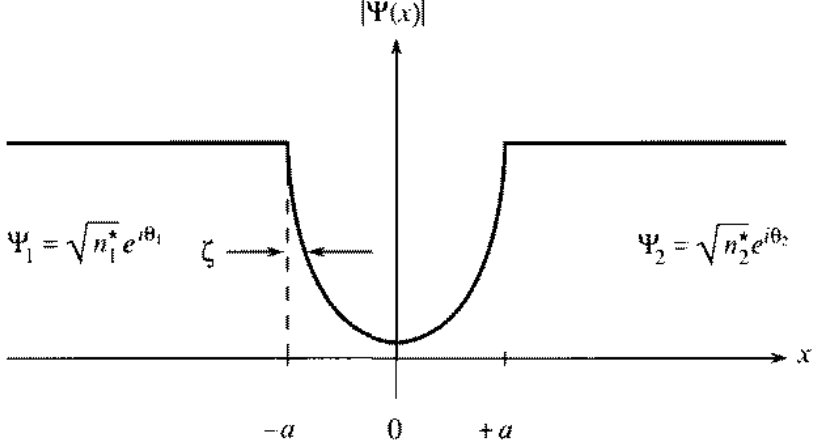


Figure 8.5 The model potential of the insulator V(x) and the magnitude of the wavefunction $|\Psi|$. The two superconductors have densities of superconducting electron pairs n_1^* and n_2^* , respectively. Furthermore, the phase of the wavefunction θ can be different for the two superconductors at $x = \pm a$.

as it travels toward the insulator. Because $V_o > \mathcal{E}_o$, the kinetic energy of the particle would have to be negative for the superelectron to be in the insulating region. However, the kinetic energy of a classical particle cannot be negative so that the superelectron is forbidden to be in the insulator. Consequently, the superelectron would not have enough energy to surmount the potential to get into in region 2, and no current would flow. Now let us see what happens quantum mechanically. Because the pairs must maintain the same energy \mathcal{E}_o the wave function can be written in terms of the time independent wavefunction $\Psi(\mathbf{r})$ of Equation 8.6. Moreover, because we are in a region of constant potential energy V_o , the time dependent Schrödingerlike equation (Equation 5.27) can be written as the time independent Schrödingerlike equation:

$$-\frac{\hbar^2}{2m^*}\nabla^2\Psi(\mathbf{r}) = (\mathcal{E}_o - V_o)\Psi(\mathbf{r}) \quad \text{for } |x| \le a.$$
 (8.7)

Our two simplifying assumptions allow us to choose a wavefunction $\Psi(x)$ that

depends only on x. The solution to Equation 8.7 for $\Psi(x)$ can be written as a sum of growing and decaying exponentials, or equivalently as

$$\Psi(x) = C_1 \cosh \frac{x}{\zeta} + C_2 \sinh \frac{x}{\zeta}, \qquad (8.8)$$

where ζ is the *decay length* in the insulator and is defined as

$$\zeta \equiv \sqrt{\frac{\hbar^2}{2m^*(V_o - \mathcal{E}_o)}}.$$
 (8.9)

This decay length ζ is considered a phenomenological parameter and is a property of the insulator and not of the superconductor. It is not to be confused with ξ , the coherence length in the superconductor. Recall from Section 5.3 that a changing wavefunction implies a supercurrent density given by (Equation 5.38)

$$\mathbf{J}_{\mathrm{s}} = \frac{q^{\star}}{m^{\star}} \operatorname{Re} \left\{ \Psi^{\star} \frac{\hbar}{i} \nabla \Psi \right\} \,.$$
 (8.10)

When the wavefunction from Equation 8.8 is put into Equation 8.10, the supercurrent density J_s simplifies to

$$\mathbf{J}_{s} = \frac{q^{*}\hbar}{m^{*}\zeta} \operatorname{Im} \{C_{1}^{*}C_{2}\}.$$
 (8.11)

Consequently, the supercurrent density across the insulator is a constant with respect to x, as expected from current continuity, and depends only on the values of C_1 and C_2 .

The coefficients C_1 and C_2 can be determined by specifying the wavefunction at the two boundaries of the insulator. Therefore, we will take

$$\Psi(-a) = \sqrt{n_1^{\star}} e^{i\theta_1} \tag{8.12}$$

and

$$\Psi(+a) = \sqrt{n_2^{\star}} e^{i\theta_2} , \qquad (8.13)$$

where $\sqrt{n_1^*}$ and θ_1 are the value of the magnitude and the phase of the wavefunction at the boundary x = -a, and similarly for the other boundary at x = a. Equating these wavefunctions with Equation 8.8 gives

$$\sqrt{n_2^{\star}}e^{i\theta_2} = C_1 \cosh\frac{a}{\zeta} + C_2 \sinh\frac{a}{\zeta}$$
 (8.14)

and

$$\sqrt{n_1^{\star}}e^{i\theta_1} = C_1 \cosh \frac{a}{\zeta} - C_2 \sinh \frac{a}{\zeta}. \tag{8.15}$$

Solving for C_1 and C_2 yields

$$C_{1} = \frac{\sqrt{n_{1}^{\star}} e^{i\theta_{1}} + \sqrt{n_{2}^{\star}} e^{i\theta_{2}}}{2 \cosh(a/\zeta)}$$
 (8.16)

and

$$C_2 = -\frac{\sqrt{n_1^*}e^{i\theta_1} - \sqrt{n_2^*}e^{i\theta_2}}{2\sinh(a/\zeta)}.$$
 (8.17)

Substitution of Equations 8.16 and 8.17 into Equation 8.11 yields the supercurrent density

$$\mathbf{J}_{\mathrm{s}} = \mathbf{J}_{\mathrm{c}} \sin \left(\theta_{1} - \theta_{2} \right). \tag{8.18}$$

Here J_c is known as the critical current density of the junction, and its magnitude is given by

$$J_c = -\frac{q^*\hbar}{m^*\zeta} \frac{\sqrt{n_1^*n_2^*}}{2\sinh(a/\zeta)\cosh(a/\zeta)} = \frac{e\hbar\sqrt{n_1n_2}}{2m\zeta\sinh(2a/\zeta)},$$
 (8.19)

where we have rewritten the values of the mass, charge, and density for a Cooper pair in terms of the parameters for an electron. Experimentally for a tunnel junction ζ is a fraction of a nanometer and typical thicknesses of the insulator is a few nanometers; that is, $2a/\zeta \gg 1$, so that $\sin 2a/\zeta \approx e^{2a/\zeta}/2$. Hence, the critical current density decreases exponentially with the thickness of the insulator. In this chapter the current density driven through the junction is always considered less than the critical current density so that only supercurrents are flowing across the junction. In Chapter 9 we show that when the driving current density exceeds the critical current of the junction that some of the current must pass through a parallel channel that is a resistive normal channel.

The fact that a supercurrent density can flow across the insulator is known as Josephson tunneling because the superelectrons are said to tunnel from one superconductor to the other through the potential V. Most importantly, Equation 8.18 shows that the supercurrent through the junction varies sinusoidally with the phase difference $\theta_1 - \theta_2$ across the junction in the absence of any scalar and vector potentials. That a difference in phase should drive a supercurrent across an insulator is somewhat expected from Equation 8.1, which states that the gradient of the phase drives a supercurrent in a single piece of superconductor. What is unexpected is that the supercurrent density in the Josephson effect goes sinusoidally with the difference in phase. This relationship between the supercurrent density and the phase is known as the Josephson current-phase relation. When the insulator is made to vanish we expect to recover the supercurrent equation for a connected piece of superconductor. In fact, for identical superconducting electrodes $n_1^* = n_2^* = n_s^*$, and taking the limit of Equation 8.18 as $a \to 0$, we get Equation 8.1 when the magnetic vector potential is zero.

The first assumption in the derivation of the current-phase relation of Equation 8.18 can now be relaxed by noting that the argument still holds if applied locally to each point on the boundary. In particular, J_o is generalized to $J_o(y,z)$, the supercurrent density at each point on the boundary of the insulator. The direction of the current density will always be considered to be in the x-direction so that there is no divergence of the current density. Consequently, for any given y and z the current will flow straight across the junction so that the corresponding wavefunction at that same y and z can still be chosen to have the dependence on x given by Equation 8.8. However, the decay length in the insulator could depend on y and z; for example, if the insulator were not made of the same material. Likewise, the thickness of the insulator 2a could also depend on y and z if the insulator were not uniform. Consequently, the critical current density given by Equation 8.18 can also depend on y and z so that the current-phase relation must be generalized to

$$\mathbf{J}_{s}(y,z,t) = \mathbf{J}_{c}(y,z)\sin\left[\theta_{1}(y,z,t) - \theta_{2}(y,z,t)\right]. \tag{8.20}$$

Unfortunately the Josephson current-phase relation of Equation 8.18 still depends on the second assumption; namely a vanishing vector potential to represent the vanishing magnetic flux density in the junction. More generally we can choose the magnetic vector potential to be written as

$$\mathbf{A}(\mathbf{r},t) = -\nabla \chi(\mathbf{r},t) \tag{8.21}$$

to ensure that $\mathbf{B} = 0$ in the junction, where $\chi(\mathbf{r}, t)$ is an arbitrary single-valued function. Now choose a new gauge

$$\mathbf{A}' = \mathbf{A} + \nabla \chi = \mathbf{0} \,, \tag{8.22}$$

so that in this gauge the vector potential vanishes. Consequently, in this gauge the current-phase relationship is the same as Equation 8.20:

$$\mathbf{J}_{\mathrm{s}} = \mathbf{J}_{\mathrm{c}} \sin \left(\theta_{\mathrm{i}}^{\prime} - \theta_{\mathrm{2}}^{\prime} \right), \tag{8.23}$$

where θ'_1 and θ'_2 are the phases of the wavefunction in the gauge with A'. In Section 5.4, we found that the phases of the wavefunctions in the two gauges are related by

$$\theta' = \theta - \frac{2\pi}{\Phi_0} \chi \,, \tag{8.24}$$

where $|q^{\star}|/\hbar$ has been replaced by $2\pi/\Phi_o$. Therefore,

$$\theta'_1 - \theta'_2 = \theta_1 - \theta_2 - \frac{2\pi}{\Phi_0} (\chi_1 - \chi_2)$$
 (8.25)

The difference of a scalar function M(r) between two points can be written as a line integral between those points by

$$M(\mathbf{r}_1) - M(\mathbf{r}_2) = -\int_{\mathbf{r}_1}^{\mathbf{r}_2} \nabla M \cdot d\mathbf{l}.$$
 (8.26)

Then the difference $(\chi_1 - \chi_2)$ can be written as a line integral from point 1 in region 1 to point 2 in region 2 of the gradient of χ so that

$$\chi_{\mathbf{i}} - \chi_{2} = -\int_{\mathbf{i}}^{2} \nabla \chi \cdot d\mathbf{l} = \int_{\mathbf{i}}^{2} \mathbf{A}(\mathbf{r}, t) \cdot d\mathbf{l}, \qquad (8.27)$$

where the gradient of χ has been written in terms of **A**. By defining $\varphi = \theta'_1 - \theta'_2$, we can write the current-phase relation as

$$\mathbf{J}_{\mathrm{S}}(\mathbf{r},t) = \mathbf{J}_{\mathrm{c}}(y,z,t)\sin\varphi(y,z,t), \qquad (8.28)$$

where φ is known as the gauge-invariant phase difference and is given by

$$\varphi(y,z,t) = \theta_1(y,z,t) - \theta_2(y,z,t) - \frac{2\pi}{\Phi_o} \int_1^2 \mathbf{A}(\mathbf{r},t) \cdot d\mathbf{l}.$$
 (8.29)

The path of integration is in the direction of the current; that is, the path is across the insulator from the superconductor with θ_1 to θ_2 , which in Figure 8.4 is from x = -a to x = +a, and the differential line element is denoted by dl.

Equations 8.28 and 8.29 have been derived in the special case when the magnetic flux density **B** vanishes in the junction. That these two relations also hold in a magnetic field can be made plausible by taking the limit as $a \to 0$ of Equation 8.28 and using Equations 8.19 and 8.29. When $n_1^* = n_2^* = n_3^*$, we recover the supercurrent equation (Equation 8.1), which is valid when **B** is nonzero. Consequently, it is plausible to assume that the current-phase relation and the gauge-invariant phase difference of Equations 8.28 and 8.29 also hold in the presence of an externally applied magnetic field, although this will not be proved here.

We now discuss the dynamics of the gauge-invariant phase difference. The time derivative of the gauge-invariant phase difference is

$$\frac{\partial \varphi}{\partial t} = \frac{\partial \theta_1}{\partial t} - \frac{\partial \theta_2}{\partial t} - \frac{2\pi}{\Phi_o} \frac{\partial}{\partial t} \int_1^2 \mathbf{A}(\mathbf{r}, t) \cdot d\mathbf{l}. \tag{8.30}$$

The substitution of the energy-phase relation (Equation 8.2) into Equation 8.30 gives

$$\frac{\partial \varphi}{\partial t} = -\frac{1}{\hbar} \left(\frac{\Lambda}{2n^{\star}} \left[\mathbf{J}_{s}^{2}(-a) - \mathbf{J}_{s}^{2}(a) \right] + q^{\star} \left[\phi(-a) - \phi(a) \right] \right)
- \frac{2\pi}{\Phi_{o}} \frac{\partial}{\partial t} \int_{1}^{2} \mathbf{A}(\mathbf{r}, t) \cdot d\mathbf{l}.$$
(8.31)

The supercurrent density is continuous so that $J_s(-a) = J_s(a)$, and

$$\frac{\partial \varphi}{\partial t} = \frac{2\pi}{\Phi_o} \int_1^2 \left(-\nabla \phi - \frac{\partial \mathbf{A}}{\partial t} \right) \cdot d\mathbf{l}. \tag{8.32}$$

The difference in the scalar potentials has been expressed as a line integral of its gradient. The term in parentheses is just the electric field E in terms of the scalar and vector potentials, as was shown in Section 5.3 (Equation 5.44). Consequently, Equation 8.32 becomes

$$\frac{\partial \varphi(y,z,t)}{\partial t} = \frac{2\pi}{\Phi_o} \int_1^2 \mathbf{E}(\mathbf{r},t) \cdot d\mathbf{l}.$$
 (8.33)

Equation 8.33 is known as the Josephson *voltage-phase relation*. Consequently, the fundamental equations governing the behavior of Josephson junctions are the current-phase relation, the gauge-invariant phase relation, and the voltage-phase relation; namely, Equations 8.28, 8.29, and 8.33, respectively. In Section 8.3, these equations are applied to some simplified junction structures and circuits.

Although the Josephson relations have been derived for a tunnel junction, they, in fact, also apply to more general types of structures. What is essential in our analysis is that the two superconducting wavefunctions interacted with each other through a region where these wavefunctions decayed spatially. In Chapter 10 we explore such structures, such as a microbridge.

8.3 BASIC LUMPED JUNCTIONS

In many interesting devices Josephson junctions can be understood by considering the gauge-invariant phase difference and the current density to be uniform over the cross section of the junction. Such a junction will be called a *basic lumped junction*. This junction can be described by a current

$$i = \int \mathbf{J} \cdot d\mathbf{s} \tag{8.34}$$

and a similarly defined critical current I_c ; the region of integration is the surface area of the junction. The current-phase relation (Equation 8.28) can be rewritten in terms of the currents:

$$i = I_c \sin \varphi(t), \qquad (8.35)$$

and the gauge-invariant phase difference is still given by

$$\varphi(t) = \theta_1(t) - \theta_2(t) - \frac{2\pi}{\Phi_o} \int_1^2 \mathbf{A}(\mathbf{r}, t) \cdot d\mathbf{l}, \qquad (8.36)$$

namely Equation 8.29. The voltage-phase relation of Equation 8.33 can be simplified by noting that $\int_1^2 \mathbf{E} \cdot d\mathbf{l}$ is just the voltage v(t) across the junction. The voltage is well defined for the lumped junction because the path of integration is well defined as being across the junction and because for a lumped junction the electric field at the terminals is independent of y and z. The voltage-phase relation then becomes

$$\frac{d\varphi}{dt} = \frac{2\pi}{\Phi_o} v \,, \tag{8.37}$$

where ν is the voltage drop across the junction in the direction of the current flow.

Note that the derivative in Equation 8.37 is a total derivative because for a lumped junction φ is independent of any spatial coordinates and depends only on time. The junction is referred to as *basic*, because the current that can be driven through the junctions is restricted not to exceed I_c so that only supercurrents flow. In Chapter 9 we discuss *generalized* junctions and how a current greater than I_c can be accommodated by an additional resistive parallel channel for normal current flow. Figure 8.6 shows the symbol for a basic lumped Josephson junction along with the two main governing equations. In this section we show that energy can be stored in a lumped junction and discuss how the lumped junction behaves when it is driven by various sources.

To find the energy of the lumped junction, consider a current source driving the junction. Let the current be slowly changed from zero to some nonzero value. Let the initial gauge-invariant phase difference φ be zero when the current is zero. As the current is slowly changed to a new steady-state value i, the gauge-invariant phase difference must also slowly change in time to reach the value consistent with the current-phase relation. When the current has reached its new value i; the voltage will be zero. However, during the time that the current slowly changed, φ had to also change. Therefore, according to the voltage-phase relation of Equation 8.37, a voltage must have been generated while φ was changing. Therefore, the current supply must have done work on the Josephson junction since an amount of power $i\nu$ was being expended by the

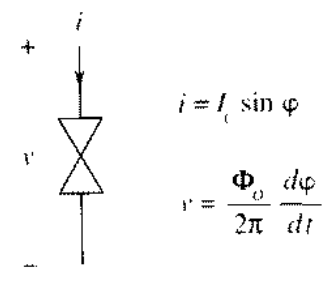


Figure 8.6 The basic Josephson junction as a lumped circuit parameter is denoted by the crossed symbol in the circuit diagram and is governed by the two equations shown.

power supply during this process. The energy W_J of the junction is then the integral of the power; namely,

$$W_J = \int_0^{t_o} iv \, dt \,. \tag{8.38}$$

Here v is the voltage generated while the current i is being changed from zero current at time t = 0 to the final value of the current at time t_o . Writing the current and voltage in terms of φ by recalling the current- and voltage-phase relations of Equations 8.35 and 8.37 yields

$$W_J = \int_0^{t_o} (I_c \sin \varphi') \left(\frac{\Phi_o}{2\pi} \frac{d\varphi'}{dt} \right) dt.$$
 (8.39)

This integral for the energy can be written as

$$W_{J} = \frac{\Phi_{o}I_{c}}{2\pi} \int_{0}^{\varphi} \sin\varphi' \,d\varphi', \qquad (8.40)$$

where φ is the phase difference associated with the driving current i and given by the current-phase relation. Direct integration gives

$$W_J = W_{Jo} - \frac{\Phi_o I_c}{2\pi} \cos \varphi \,, \tag{8.41}$$

and here $W_{Jo} = \Phi_o I_c/2\pi$ is a constant. Figure 8.7 plots the difference in energy and the current of the junction as a function of the gauge-invariant phase difference. The energy is lowest when no current flows and φ is a multiple of 2π .

Having found the governing current-phase and voltage-phase relations as well as the energy stored in the basic lumped junction, we now discuss the dynamics of the junction. If the lumped junction is driven by a time dependent

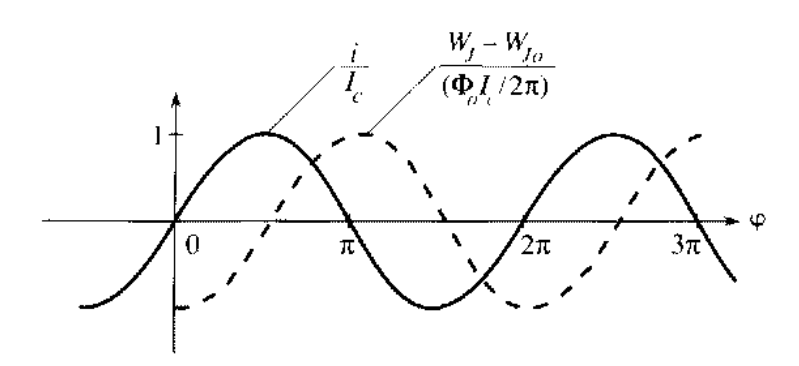


Figure 8.7 The current *i* and the energy difference $W_I - W_{Jo}$ as a function of the gauge-invariant phase difference across a basic Josephson junction.

current, this current creates a time dependent φ given by the current-phase relation, and thereby generates a voltage according to the voltage-phase relation. On the other hand, if the lumped junction is driven by a voltage, the dynamics can be more complex and we now turn our attention to this situation.

When a voltage v(t) is driven across a basic lumped Josephson junction, the gauge-invariant phase difference changes in time according to the Josephson voltage-phase relation, namely, Equation 8.37. If the driving voltage is a constant V_o , then φ increases linearly in time as

$$\varphi(t) = \varphi(0) + \frac{2\pi}{\Phi_o} V_o t. \tag{8.42}$$

Consequently, using the current-phase relationship of Equation 8.35, we see that an ac current

$$i = I_c \sin \left[\frac{2\pi}{\Phi_o} V_o t + \varphi(0) \right]$$
 (8.43)

$$=I_c\sin\left[2\pi f_I t + \varphi(0)\right] \tag{8.44}$$

develops across the junction. This effect is known as the ac Josephson effect and f_J is the Josephson frequency, given by

$$f_J = \frac{V_o}{\Phi_o} = \frac{2e}{h} V_o = 483.6 \times 10^{12} V_o \text{ (Hz)}.$$
 (8.45)

The corresponding time constant for a basic Josephson junction is then f_J^{-1} .

For a constant driving voltage of 10 μ V, the current will oscillate at about 5 GHz. Because a few microvolts is typical of the lower voltage range applied to a Josephson junction, we see that we are generally operating at frequencies in the microwave regime. In some circuits at these frequencies care must be taken in considering other parts of the circuit as lumped circuit elements. For example, waveguides, which are not lumped circuit elements, are often used in the microwave circuitry with Josephson junctions. In addition, at these high frequencies the junction can emit radiation. Because the Josephson junction is similar to the same waveguide structure that we considered in Section 4.4, it is not surprising that the emitted radiation is greatest when the Josephson frequency is a resonant frequency of the structure. The power of the emitted radiation for a single junction is usually less than a microwatt and detection is hampered by the impedance mismatch between free space and the waveguide structure. It is interesting to note that the reciprocal phenomena holds: radiation can be coupled to an unbiased Josephson junction, causing the inverse ac Josephson effect in which a dc voltage appears across the junction.

We have found that a constant driving voltage generates an ac current in

a Josephson junction. Now consider the case of a driving voltage that is time dependent. In particular, let

$$v(t) = V_o + V_s \cos \omega_s t. \tag{8.46}$$

From the integration of the voltage-phase relation (Equation 8.37), the gauge-invariant phase difference is found to vary in time as

$$\varphi(t) = \varphi(0) + \frac{2\pi}{\Phi_o} V_o t + \frac{2\pi V_s}{\Phi_o \omega_s} \sin \omega_s t. \qquad (8.47)$$

From the current-phase relation, this phase results in the current varying as

$$i = I_c \sin \left(\varphi(0) + \frac{2\pi}{\Phi_o} V_o t + \frac{2\pi V_s}{\Phi_o \omega_s} \sin \omega_s t \right). \tag{8.48}$$

The frequency of the current is the superposition of a constant frequency $f_J = V_o/\Phi_o$ and a sinusoidally varying phase. Therefore, the frequency of the current response is not the same frequency as the driving voltage. This is because the nonlinear current-phase relation can couple different frequencies with the driving frequency. Although the resulting current has a complicated dependence on time, it is similar to the dependence on frequency found in FM signal analysis. To get a better understanding of the time dependence of the current, we rewrite Equation 8.48 as a Fourier series. This can be accomplished with the aid of the Fourier-Bessel series identity

$$e^{ib\sin x} = \sum_{n=-\infty}^{+\infty} [J_n(b)]e^{inx},$$
 (8.49)

where J_n is the *n*th order Bessel function of the first kind. To apply this identity, note that the argument of the first sine function in Equation 8.48 is of the form $(a + b \sin x)$ so that

$$\sin\left(a+b\sin x\right)=\operatorname{Im}\left\{e^{i\left(a+b\sin x\right)}\right\} \ . \tag{8.50}$$

The Fourier-Bessel series identity along with the fact that

$$J_{-n}(b) = (-1)^n J_n(b)$$
 (8.51)

allows us to write

$$e^{i(a+b\sin x)} = \sum_{n=-\infty}^{+\infty} J_n(b) e^{i(a+nx)} = \sum_{n=-\infty}^{+\infty} (-1)^n J_n(b) e^{i(a-nx)}.$$
 (8.52)

Consequently, the imaginary part of Equation 8.52 gives

$$\sin(a + b\sin x) = \sum_{n = -\infty}^{+\infty} (-1)^n J_n(b) \sin(a - nx).$$
 (8.53)

Therefore, the current in Equation 8.48 can be written as

$$i = I_c \sum_{n=-\infty}^{\infty} (-1)^n \left[J_n \left(\frac{2\pi V_s}{\Phi_o \omega_s} \right) \right] \sin \left[(2\pi f_J - n\omega_s)t + \varphi(0) \right].$$
 (8.54)

This series shows that the nonlinear current-phase relation gives a current response in which the frequency f_I due to the dc part of the driving voltage couples to multiples of the driving frequency ω_s . Again $|i| \leq I_c$ must be satisfied for the analysis with the basic junction to be valid (so that only supercurrents flow in the circuit); the more general case will be taken up in the next chapter.

Of particular interest is the fact that the current response can be at zero frequency even when the driving voltage is at a nonzero frequency; that is, an ac voltage drive can result in a dc current response. This dc current will occur when the argument of the sine term in Equation 8.54 vanishes; namely, when $2\pi f_J = n\omega_s$ or, equivalently when

$$V_o = n \left(\frac{\Phi_o}{2\pi}\right) \omega_s. \tag{8.55}$$

For a particular n the average dc current $\langle i \rangle$ must satisfy

$$|\langle i \rangle| \leq I_c J_n \left(\frac{2\pi V_s}{\Phi_o \omega_s}\right)$$
, (8.56)

the exact value depending on the initial value $\varphi(0)$. When a driving voltage at 1 GHz is applied across the junction for various values of V_o , a constant dc current will appear at $V_o = 0$ and at integral multiples of about $2 \mu V$. This spacing in the values V_o that gives a constant current response is expected between neighboring values of n in Equation 8.55. Let this voltage spacing be denoted by δv . Note that the relationship between δv and the applied frequency, $f_s = \omega_s/2\pi$, depends only on fundamental constants; namely, from Equation 8.55, $\delta v = (h/2e)f_s$.

8.4 SUPERCONDUCTING QUANTUM INTERFERENCE

Two Josephson junctions can be combined in parallel to produce a device known as a superconducting quantum interference device (SQUID), which is a sensitive detector of magnetic flux. Figure 8.8 shows two such identical basic

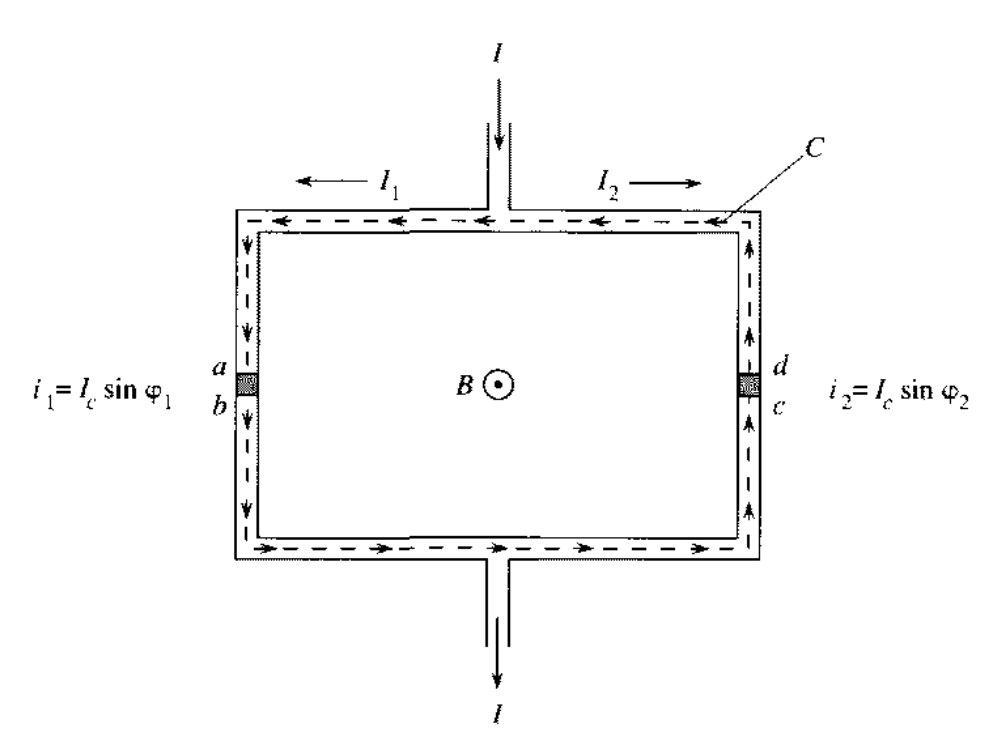


Figure 8.8 Two Josephson junctions connected in parallel by superconducting wire. The path of integration *C* is shown by the dotted line.

lumped Josephson junctions connected in parallel and joined by superconducting wire. The first junction is characterized by $i_1 = I_c \sin \varphi_1$ and the second by $i_2 = I_c \sin \varphi_2$. The total current i is

$$i = i_1 + i_2 = I_c \sin \varphi_1 + I_c \sin \varphi_2 \tag{8.57}$$

$$=2I_{c}\cos\left(\frac{\varphi_{1}-\varphi_{2}}{2}\right)\sin\left(\frac{\varphi_{1}+\varphi_{2}}{2}\right). \tag{8.58}$$

The difference in the gauge invariant phases can be found by integrating $\nabla \theta$ around the closed path C shown in Figure 8.8 and noting that θ is a multivalued function that can change by $2\pi n$ upon completing the path, where n is an integer. Carrying out the integration we have

$$\oint_C \nabla \theta \cdot d\mathbf{l} = 2\pi \mathbf{n} \tag{8.59}$$

$$= (\theta_b - \theta_a) + (\theta_c - \theta_b) + (\theta_d - \theta_c) + (\theta_a - \theta_d).$$
 (8.60)

where the integral has been divided into four terms consisting of differences of phases. The first and the third term are differences across the Josephson

junctions and follow directly from the definition of the gauge-invariant phase difference in Equation 8.29; namely,

$$\theta_b - \theta_a = -\varphi_1 - \frac{2\pi}{\Phi_o} \int_a^b \mathbf{A} \cdot d\mathbf{l}$$
 (8.61)

and

$$\theta_d - \theta_c = \varphi_2 - \frac{2\pi}{\Phi_0} \int_0^d \mathbf{A} \cdot d\mathbf{l}. \qquad (8.62)$$

The second and the fourth terms are differences in the superconducting wire itself and are found by using the supercurrent equation for $\nabla \theta$ in Equation 8.1:

$$\theta_c - \theta_b = \int_b^c \nabla \theta \cdot d\mathbf{l} = -\frac{2\pi}{\Phi_o} \int_b^c \Lambda \mathbf{J} \cdot d\mathbf{l} - \frac{2\pi}{\Phi_o} \int_b^c \mathbf{A} \cdot d\mathbf{l}$$
 (8.63)

and

$$\theta_a - \theta_d = \int_d^a \nabla \theta \cdot d\mathbf{l} = -\frac{2\pi}{\Phi_o} \int_d^a \Lambda \mathbf{J} \cdot d\mathbf{l} - \frac{2\pi}{\Phi_o} \int_d^a \mathbf{A} \cdot d\mathbf{l}.$$
 (8.64)

Substitution of Equations 8.61-8.64 into Equation 8.60 gives

$$\varphi_2 - \varphi_1 = 2\pi \mathbf{n} + \frac{2\pi}{\Phi_o} \oint_C \mathbf{A} \cdot d\mathbf{l} + \frac{2\pi}{\Phi_o} \int_b^c \Lambda \mathbf{J} \cdot d\mathbf{l} + \frac{2\pi}{\Phi_o} \int_d^a \Lambda \mathbf{J} \cdot d\mathbf{l}. \quad (8.65)$$

Note that the integration of A is around a complete closed contour C and is equal to the total flux Φ inside the area enclosed by the contour. The integration of J follows the same path as the contour C but excludes the integration over the insulators; for convenience this integration will be denoted compactly by

$$\int_{C'} \Lambda \mathbf{J} \cdot d\mathbf{l} \equiv \int_{b}^{c} \Lambda \mathbf{J} \cdot d\mathbf{l} + \int_{d}^{a} \Lambda \mathbf{J} \cdot d\mathbf{l}, \qquad (8.66)$$

where C' is an incomplete path that follows C but excludes the insulators. The difference in the gauge-invariant phase differences can then be written as

$$\varphi_2 - \varphi_1 = 2\pi \mathbf{n} + \frac{2\pi\Phi}{\Phi_o} + \frac{2\pi}{\Phi_o} \int_{C'} \Lambda \mathbf{J} \cdot d\mathbf{l}$$
 (8.67)

If the superconducting wire is thicker than a few penetration depths, then the path of integration can be taken deep inside the superconducting wires where the integral involving the current density is negligible. Equation 8.67 then simplifies to relate the phase difference to the total flux by

$$\varphi_2 - \varphi_1 = 2\pi n + \frac{2\pi\Phi}{\Phi_0}. \tag{8.68}$$

The total current as given in Equation 8.58 becomes

$$i = 2I_c \cos\left(\frac{\pi\Phi}{\Phi_o}\right) \sin\left(\varphi_1 + \frac{\pi\Phi}{\Phi_o}\right). \tag{8.69}$$

Let the inductance of the loop be L. The total flux becomes the sum of the externally applied flux $\Phi_{\rm ext}$, and the flux generated by currents flowing in the loop. We have restricted ourselves to having the two junctions and the two sides of the loop as identical. The currents can be written as

$$i_1 = \hat{I} + I_{\text{cir}} \tag{8.70}$$

and

$$i_2 = \bar{I} - I_{\rm cir}$$
 (8.71)

Here $\bar{I} = (i_1 + i_2)/2$ is the average current common to both currents and hence generates no net flux in the loop. On the other hand, $I_{\rm cir} = (i_1 - i_2)/2$ is the circulating current and generates a flux $LI_{\rm cir}$. The total flux is then

$$\Phi = \Phi_{\rm ext} + LI_{\rm cir} \tag{8.72}$$

$$=\Phi_{\rm ext}+\frac{LI_c}{2}\left(\sin\varphi_1-\sin\varphi_2\right) \tag{8.73}$$

$$=\Phi_{\rm ext}+LI_c\,\sin\!\left(\frac{\varphi_1-\varphi_2}{2}\right)\cos\!\left(\frac{\varphi_1+\varphi_2}{2}\right). \tag{8.74}$$

Using Equation 8.68, we can write the total flux as an implicit function of Φ_{ext} and φ_{L} ,

$$\Phi = \Phi_{\rm ext} - LI_c \sin\left(\frac{\pi\Phi}{\Phi_o}\right)\cos\left(\varphi_1 + \frac{\pi\Phi}{\Phi_o}\right).$$
 (8.75)

In summary, Equations 8.69 and 8.75 must be solved self-consistently to describe the behavior of the SQUID. We first consider the case when the inductance is negligible so that the total flux is just the applied flux; then the more general case is considered. In all cases we seek the maximum driving current i_{max} that can be sent through the SQUID such that the current through each junction does not exceed the critical current of each junction. This current is important since for $|i| \leq i_{\text{max}}$, each junction will be operating as a basic junction that is consistent with the initial assumptions of this chapter. If $|i| > i_{\text{max}}$, then, as is shown in Chapter 9, some of the current must flow through a parallel normal tunneling channel and some resistance will appear across the junction. Therefore, i_{max} delineates the regions between seeing no resistance and seeing a resistance in the SQUID. The onset of this resistance can be detected as the

driving current exceeds i_{max} , so that the value of i_{max} is an important device parameter that forms the basis of operating a SQUID.

The Special Case $LI_c \ll \Phi_{\rm ext}$. When the flux produced by the circulating current is negligible, the total flux is the externally applied flux $\Phi_{\rm ext}$. This condition will hold as long as $LI_c \ll \Phi_{\rm ext}$. At a given $\Phi_{\rm ext}$, the current $i_{\rm max}$ is found by maximizing Equation 8.69 with respect to φ_1 as follows. The extremum of the current occurs when the derivative of the current in Equation 8.69 with respect to φ_1 vanishes, which happens when

$$\cos\left(\varphi_1 + \pi \Phi_{\text{ext}}/\Phi_o\right) = 0. \tag{8.76}$$

Thus, at the extremum

$$\sin\left(\varphi_1 + \pi \Phi_{\text{ext}}/\Phi_o\right) = \pm 1 \,, \tag{8.77}$$

and the maximum value of i is found by taking the sign of the sine term so that the current is positive. This results in

$$i_{\max} \approx 2I_c \left| \cos \left(\frac{\pi \Phi_{\rm ext}}{\Phi_o} \right) \right| \,, \tag{8.78}$$

which is periodic in the external flux as shown in Figure 8.9. If the area enclosed by the SQUID is $2 \, \text{cm}^2$, then the current is periodic for every $10 \, \text{pT}$ ($10^{-11} \, \text{T}$). With the use of pick-up coils to transport the flux from near a human body to a SQUID detector, magnetic fields generated by the human brain ($\sim 1 \, \text{fT}$) can be measured. Magnetometers based on SQUIDs are discussed further in Section 9.5.

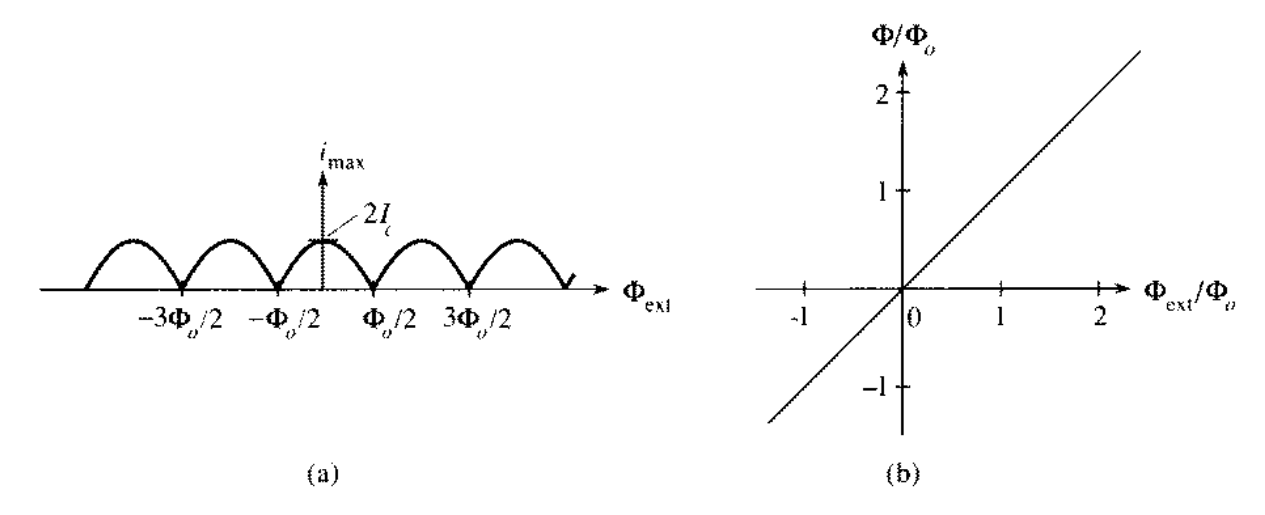


Figure 8.9 (a) $i_{\rm max}$ versus $\Phi_{\rm ext}$ for identical Josephson junctions in parallel when the self-induced flux is neglected so that $\Phi \approx \Phi_{\rm ext}$ as in (b).

The General Case. In general, both the external flux and the flux due to the circulating current comprise the total flux so that Equation 8.75 is satisfied. The maximum current i_{max} that can be sent through the SQUID at a given $\Phi_{\rm ext}$ is again found by maximizing Equation 8.69 with respect to φ_1 , with the constraint given by Equation 8.75. This problem has been solved numerically by de Bruyn Ouboter and de Waele and some of the results are shown in Figures 8.10 and 8.11. We see that for the value of the inductance chosen that the modulation of the critical current is reduced in comparison to the modulation shown in Figure 8.9 for negligible inductance. Furthermore, the total flux begins to become a steplike function of the applied flux in contrast to being equal to the applied flux as when $LI_c \ll \Phi_{\rm ext}$. To understand this behavior we note that for large enough inductances such that $LI_c \gg \Phi_{\rm ext}$, the circulating current will tend to cancel the applied flux. The loop of the SQUID will look more and more like the single loop of superconducting wire that was studied in Section 5.5. Consequently, the total flux in the loop will tend to be quantized as

$$\Phi = \Phi_{\rm ext} + LI_{\rm cir} \approx n\Phi_{\rm o} \,, \tag{8.79}$$

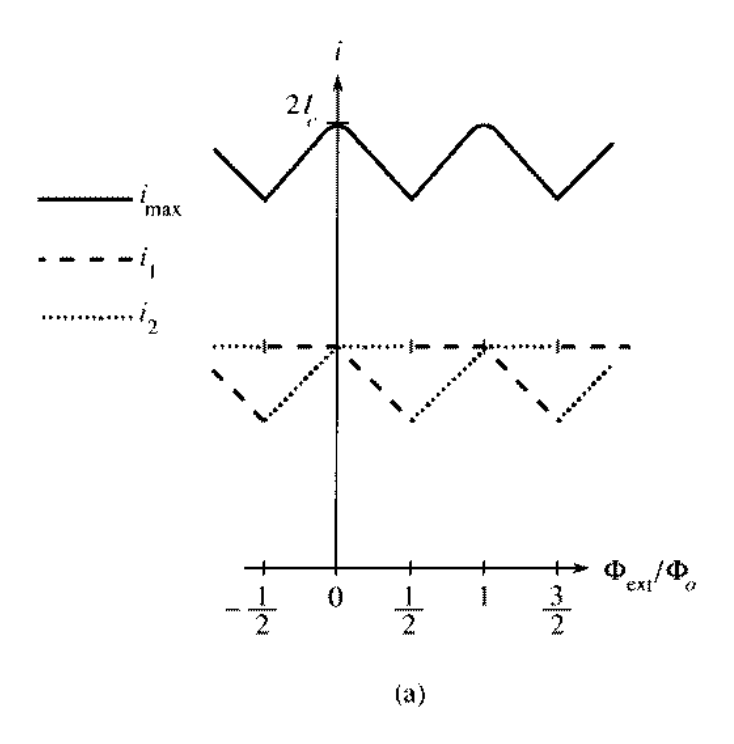
where n is the integer closest to $\Phi_{\rm ext}/\Phi_o$. This means that the total flux will follow the staircase pattern as a function of the external flux as shown in Figure 5.3. In Section 5.5 we showed that this staircase pattern was a result of minimizing the energy of the superconducting loop. We found that a loop cooled in a field was described by this behavior, but that the dynamical equations for a single loop made the flux constant as a function of applied flux when the loop was already superconducting. Therefore, we see that a superconducting loop with a Josephson junction behaves differently than a superconducting loop. The reason that the Josephson junction always maintains the lowest energy state is that $\varphi_{\rm f}$ is free to assume any value. Therefore, the circulating current becomes

$$I_{\rm cir} pprox - rac{\Phi_{
m ext} - n\Phi_o}{L},$$
 (8.80)

which tends to zero as L increases. With this negligibly small circulating current, the applied current divides nearly equally down both paths. The maximum applied current will then occur when I_c goes through each junction so that $i_{\rm max}\approx 2I_c$ for all applied fields. To see why $i_{\rm max}$ has a small deviation from $2I_c$, consider the flux being increased initially from zero. A small circulating current will flow to oppose the flux so that

$$I_{\rm cir} \approx -\frac{\Phi_{\rm ext}}{I_{\rm c}}$$
, (8.81)

when n is zero initially. Therefore, the current i_1 will tend to decrease while the current i_2 will tend to increase. However, i_2 cannot increase beyond I_c so



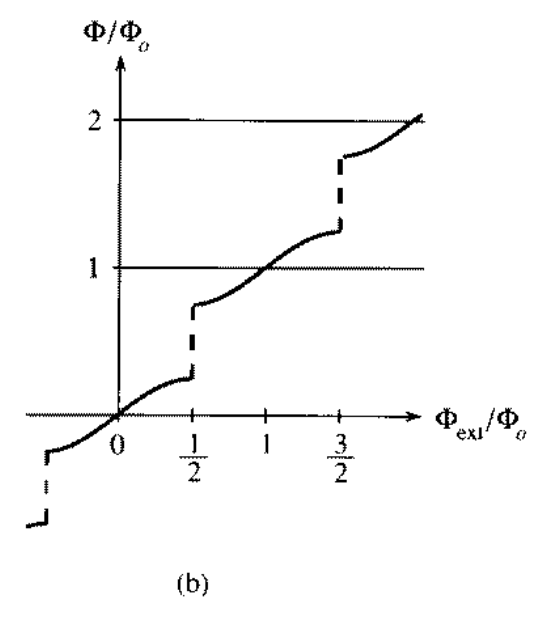


Figure 8.10 (a) i_{max} versus Φ_{ext} for identical Josephson junctions in parallel when $LI_c = 5\Phi_o/\pi$. The currents through the two junctions when $i = i_{\text{max}}$ are denoted as i_1 and i_2 . (b) The total flux versus the applied flux Φ_{ext} . Source: R. de Bruyn Ouboter and A. Th. A. M. de Waele, "Superconducting Point Contacts Weakly Connecting Two Superconductors," from Progress in Low Temperature Physics, Vol. VI, edited by C. J. Gorter. Copyright © 1970 by Elsevier Science Publishers. Reprinted with permission.

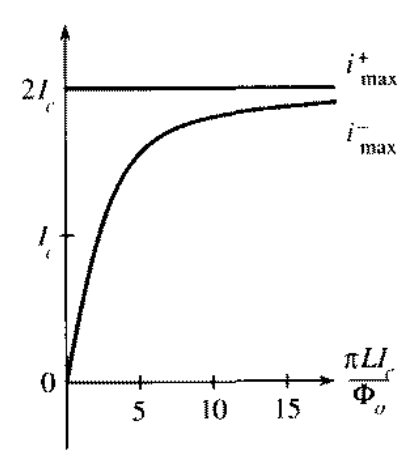


Figure 8.11 The upper (i_{max}^+) and lower (i_{max}^-) bounds of the modulation of i_{max} as a function of the inductance. The plot is in reduced units of $\pi LI_c/\Phi_o$. Source: R. de Bruyn Ouboter and A. Th. A. M. de Waele, "Superconducting Point Contacts Weakly Connecting Two Superconductors," from Progress in Low Temperature Physics, Vol. VI, edited by C. J. Gorter. Copyright © 1970 by Elsevier Science Publishers. Reprinted with permission.

it will be fixed at I_c as i_1 decreases. Specifically because $i_1 = i_2 + 2I_{cir}$ then i_1 decreases as

$$i_1 \approx I_c - \frac{2\Phi_{\rm ext}}{L},\tag{8.82}$$

as i_2 remains fixed at I_c . This behavior is shown in Figure 8.10 as the external flux is increased from zero and is less than $\Phi_o/2$. When the external flux exceeds $\Phi_o/2$, then n=1 and the circulating current changes sign so that the roles of i_1 and i_2 are reversed, and this reversal happens periodically with every $\Phi_o/2$. With these values of i_1 and i_2 the modulation of the total maximum current can then be approximated as

$$i_{\text{max}} \approx 2I_c - \frac{2|\Phi_{\text{ext}} - n\Phi_o|}{L}$$
 (8.83)

Figure 8.11 shows i_{max}^- and i_{max}^+ , which are the lowest and highest to which i_{max} can be modulated by the external flux. Consequently, for large inductances the maximum modulation in the current is

$$i_{\text{max}}^+ - i_{\text{max}}^- \approx \frac{\Phi_o}{L}, \qquad (8.84)$$

because $i_{\text{max}}^+ = 2I_c$ and i_{max}^- occurs when the external flux differs from an integral number of flux quantum by a half of a flux quantum.

A graphical method will now be given that allows one to pictorially account for what the total current and energy is in the SQUID as well as in each individual junction. First we rewrite two of the governing equations for a single Josephson junction as follows:

$$i = I_c \sin \varphi \tag{8.85}$$

and

$$\frac{2\pi(W-W_{Jo})}{\Phi_o = -I_c\cos\varphi}.$$
 (8.86)

These equations can be represented as components of a two-dimensional phasor (vector) as shown in Figure 8.12. The phasor has a magnitude I_c and the angle it makes with the negative vertical axis is the gauge-invariant phase difference φ . The projection of the phasor on the horizontal-axis is the current across the junction and hence we refer to the horizontal axis as the current axis. Likewise, the projection of the phasor on the vertical axis is equal to $2\pi(W-W_{Jo})/\Phi_o$, which is proportional to the difference in the energy. The vertical axis is referred to as the energy axis.

The phasors are particularly useful in analyzing the two junction SQUID, as in Figure 8.8. There the total current i is just the sum of the individual currents

$$i = I_{c1} \sin \varphi_1 + I_{c2} \sin \varphi_2$$
, (8.87)

where the two junctions are now allowed to be different. Consequently, if the two currents are represented as phasors, as shown in Figure 8.13, then their vector sum would have a projection on the current axis that satisfies Equation 8.87. The difference in energy is also the sum of the differences of each junction, namely,

$$\frac{2\pi(W - W_{Jo})}{\Phi_o} = -I_{c1}\cos\varphi_1 - I_{c2}\cos\varphi_2.$$
 (8.88)

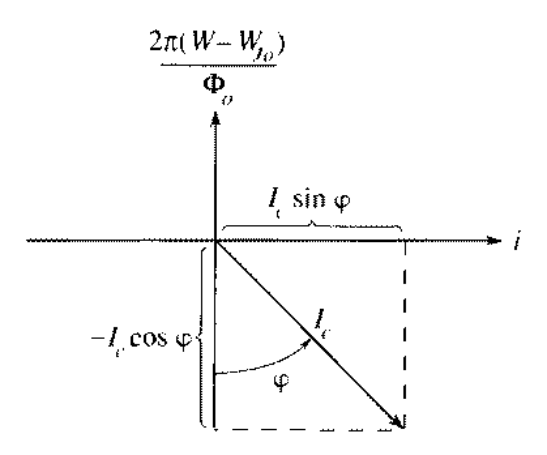


Figure 8.12 The Josephson Phasor

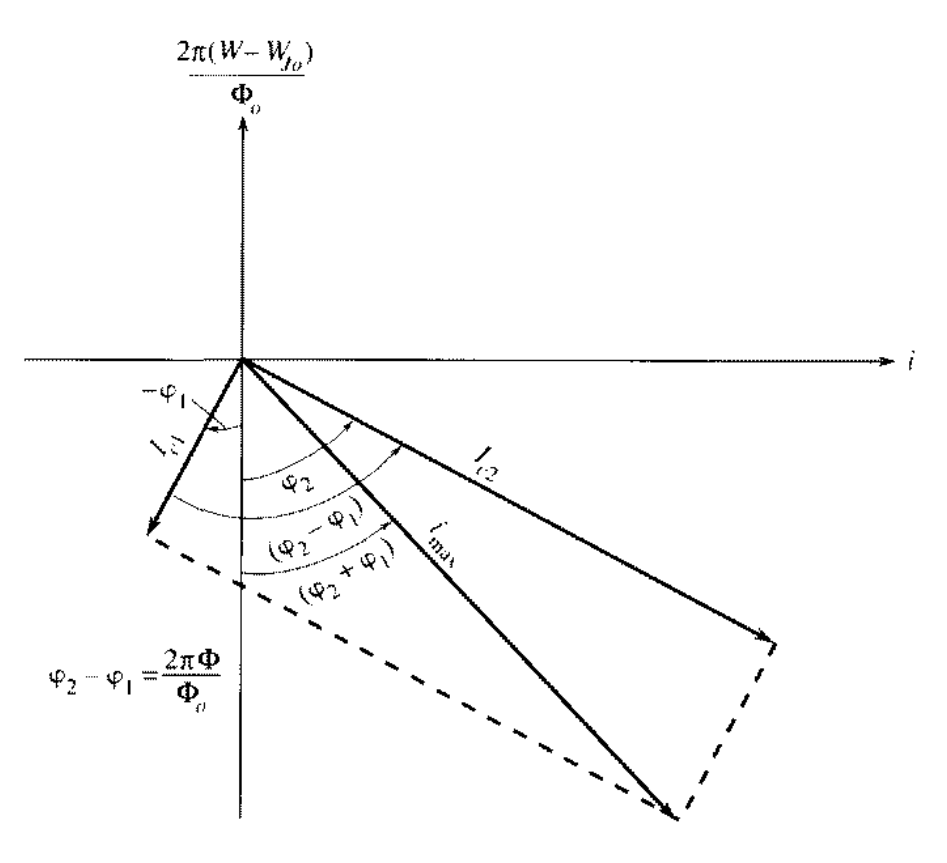


Figure 8.13 The Josephson Phasors for a SQUID with Two Different Junctions

The projection of the resultant vector on the energy axis in Figure 8.13 also satisfies the above equation. For the two junction SQUID the difference in the gauge-invariant phase differences is related to the total flux by Equation 8.68, which we repeat here:

$$\varphi_2 - \varphi_1 = 2\pi n + \frac{2\pi\Phi}{\Phi_o}. \tag{8.89}$$

The phasor construction in Figure 8.13 shows that although the difference in the phases is fixed by the flux, the sum of the phases can be made to vary. Moreover, the sum of the phases $\varphi=(\varphi_1+\varphi_2)$ is just the phase of the resultant vector. When no current i is applied, the resultant vector is parallel to the energy axis and has its phase set to zero. As the applied current is increased, the resultant phase increases and reaches a maximum at $\varphi=\pi/2$ so that the resultant vector is parallel to the current axis. The magnitude of the maximum current that can be sent through the SQUID is just the magnitude of the resultant vector. Therefore,

$$i_{\text{max}} = \sqrt{I_{c1}^2 + I_{c2}^2 + 2I_{c1}I_{c2}\cos\frac{2\pi\Phi}{\Phi_o}}$$
, (8.90)

where Equation 8.89 has been used to express the difference between the individual phases. In general, Equation 8.90 must be solved self-consistently with the total flux in the loop (Equation 8.75), a procedure that must be solved numerically as before. However, when the inductance is small enough such that $LI_c \ll \Phi_{\rm ext}$, the total flux is just the applied flux in Equations 8.89 and 8.90. For identical junctions, Equation 8.90 is equivalent to the previous expression found for the maximum current; namely, Equation 8.78.

The Josephson phasors also give a good picture of the ac Josephson effect. The phasor is initially at some angle $\varphi(0)$ as shown in Figure 8.12. The applied voltage V_o causes the phase to increase at a constant rate so that the phasor rotates at a constant angular frequency $2\pi f_I$. Thus the projection of the phasor on the current axis varies sinusoidally in accord with Equation 8.44. Also the difference in energy changes sinusoidally with the same frequency but -90° out of phase with the current.

8.5 SHORT JOSEPHSON JUNCTIONS

Thus far we have considered the Josephson junction as a lumped circuit element where the gauge-invariant phase difference and the current density are considered uniform throughout the area of the junction. In Sections 8.5 and 8.6 we generalize to cases where the gauge-invariant phase difference and the current density through the junction can vary, and we shall refer to such junctions as extended Josephson junctions. The behavior of extended Josephson junctions in a magnetic field forms the basis of single junction SQUIDs and also the switching scheme in most logic and memory circuits.

In this section we analyze the behavior of extended Josephson junctions in a magnetic field by first assuming that the magnetic field produced by the currents through the junction is negligible in comparison to the externally applied magnetic field. Such junctions are referred to as *short* junctions. We find that a single short junction can produce an interference pattern and that vortices can exist in the junction and cause dissipation. The analysis of the energy stored in the junction reveals a new characteristic length scale. The short junction then is more precisely defined as a junction whose length and width are small compared to this characteristic length. In Section 8.6 we analyze the behavior of long Josephson junctions, where long indicates that the length of the junction is longer than the characteristic length, and we show that self-fields are then important. Long Josephson junctions have many of the same general features of short junctions but with the additional constraint that the fields and currents decay away from the center of the vortex on a length scale of the characteristic length; hence this length is called the Josephson penetration depth λ_J .

Consider the cross section of a Josephson junction as shown in Figure 8.14. The two superconductors are separated by an insulating barrier of thickness 2a. Each superconductor has a thickness, b_1 and b_2 , which is much larger than its respective penetration depth λ_1 and λ_2 . The superconductors extend a length d

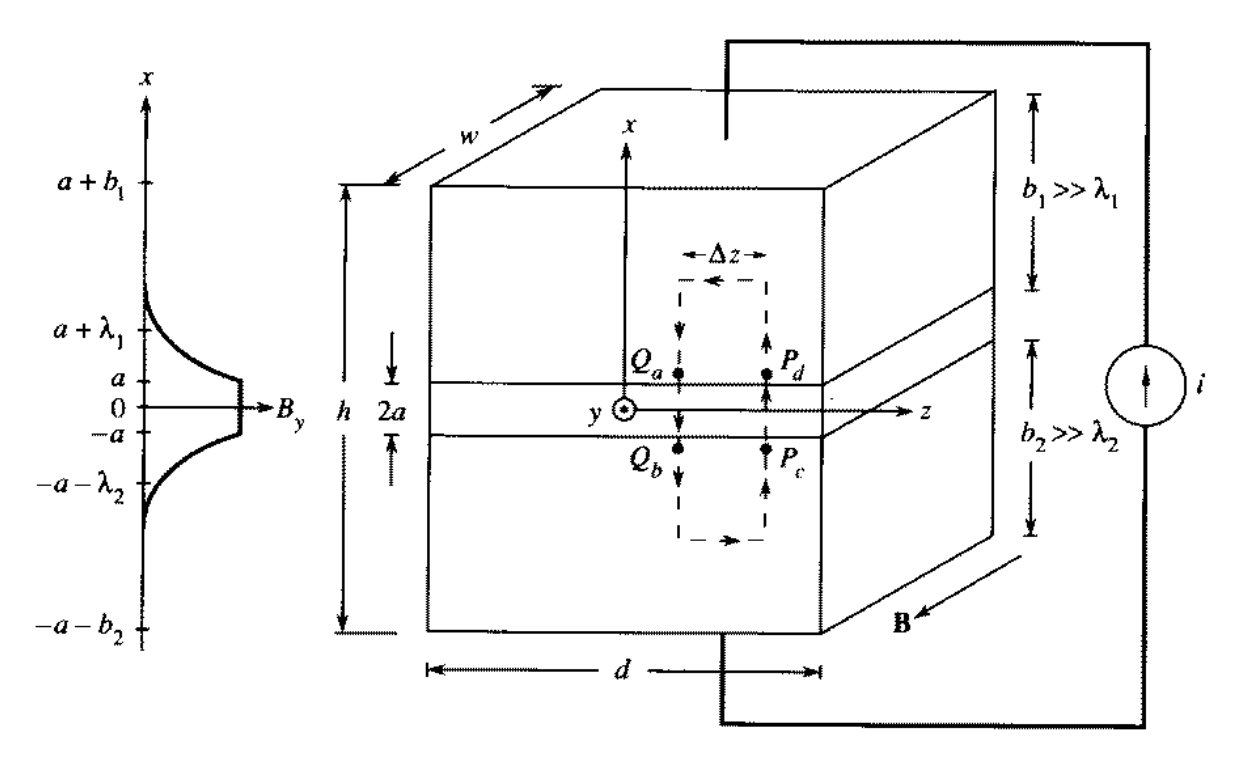


Figure 8.14 The cross section of a Josephson junction. The current flows across the junction in the -x-direction.

in the z-direction and a width w in the y-direction. We will take $d \gg 2a$ and $w \gg 2a$ so that effects due to the edges will be ignored. The externally applied magnetic flux density is in the y-direction so that $\mathbf{B} = B_o \mathbf{i}_v$ and B_o is constant.

Now consider two points Q and P, which are an infinitesimal distance Δz apart along the z-axis, which is taken to be in the center of the insulator. The gauge-invariant phase difference between the two points is found by considering the contour in Figure 8.14. An analysis identical to that of the SQUID with two lumped junctions can be made by letting the points a, b, c, and d in Figure 8.14 correspond to the same labeled points in Figure 8.8. This analysis results in the same relationship; namely, Equation 8.67. Consequently,

$$\varphi(P) - \varphi(Q) = 2\pi \mathbf{n} + \frac{2\pi}{\Phi_o} \oint_C \mathbf{A} \cdot d\mathbf{l} + \frac{2\pi}{\Phi_o} \int_{C'} \Lambda \mathbf{J} \cdot d\mathbf{l}$$
 (8.91)

$$=2\pi\mathbf{n}+\frac{2\pi\Phi}{\Phi_o}+\frac{2\pi}{\Phi_o}\int_{C'}\Lambda\mathbf{J}\cdot d\mathbf{l},\qquad \qquad \mathbf{(8.92)}$$

where Φ is the total flux inside the area of the integration path C and $\int_{C'} \Lambda \mathbf{J} \cdot d\mathbf{l}$ is an integration over the same path but excluding the insulator. The integration of the current density along one segment of the path in the x-direction cancels with the contribution of the adjacent path, which is an infinitesimal distance Δz away. Each part of the path in the z-direction is taken many penetration depths away from the surface of each superconductor. There the currents induced by the external magnetic field will be exponentially small so that the only current density is the applied current. But the applied current is in the

negative x-direction, so it is perpendicular to the direction of the path and, hence, contributes nothing to the integral of the current density. Therefore, the line integral of the current density vanishes so that the difference in the gauge-invariant phase differences becomes

$$\varphi(P) - \varphi(Q) = \frac{2\pi\Phi}{\Phi_o},$$
(8.93)

where the phase difference is measured modulo 2π . Furthermore, the magnetic field decays exponentially into each superconducting slab so that the total flux enclosed is

$$\Phi = B_{\nu}(\lambda_1 + \lambda_2 + 2a) \Delta z. \qquad (8.94)$$

Now

$$\varphi(P) - \varphi(Q) = \frac{\partial \varphi}{\partial z} \Delta z$$
, (8.95)

so that in the limit of infinitesimal Δz , Equations 8.93 and 8.94 give

$$\frac{\partial \varphi}{\partial z} = \frac{2\pi}{\Phi_o} B_y h_{\text{eff}} \,, \tag{8.96}$$

where

$$h_{\text{eff}} = \lambda_1 + \lambda_2 + 2a. \tag{8.97}$$

A similar argument can be made by choosing the point P to be an infinitesimal distance Δy in the y-direction to give

$$\frac{\partial \varphi}{\partial y} = -\frac{2\pi}{\Phi_o} B_z h_{\text{eff}}, \qquad (8.98)$$

where care has been taken with regards to the direction of the contour and the direction of the magnetic field. Both Equations 8.96 and 8.98 state that the phase changes in a certain direction only if there is a component of the magnetic field perpendicular to that direction.

For short junctions we, by assumption, neglect the self-fields from the currents and take $\mathbf{B} = B_o \mathbf{i}_y$. The phase then does not change in the y-direction so that $\varphi = \varphi(z)$. Equation 8.96 integrates directly to give

$$\varphi(z) = \frac{2\pi}{\Phi_o} B_o h_{\text{eff}} z + \varphi(0) , \qquad (8.99)$$

where $\varphi(0)$ is a constant and is the phase at the origin. The resulting supercurrent density in the insulator is in the x-direction and is given by the current-phase relation of Equation 8.28 so that

$$J_{s}(y,z,t) = J_{c}(y,z)\sin\varphi(z,t). \tag{8.100}$$

Furthermore, the total current through the junction is

$$i = \int_{-d/2}^{d/2} \int_{-w/2}^{w/2} J_s(y, z) \, dy \, dz \,. \tag{8.101}$$

Let the critical current density be a constant J_c over the area of the junction so that Equation 8.101 integrates simply to

$$i\left(\Phi_{J},\varphi(0)\right) = I_{c} \frac{\sin\frac{\pi\Phi_{J}}{\Phi_{o}}}{\frac{\pi\Phi_{J}}{\Phi_{o}}} \sin(\varphi(0)).$$
 (8.102)

Here $\Phi_J = B_o h_{\rm eff} d$ is the flux through the junction, and $I_c = J_c wd$ is the maximum critical current through the junction and the same critical current as for a lumped junction. Hence we see that the total supercurrent depends not only on the flux through the junction but also on the integration constant $\varphi(0)$. Just as in the case of SQUID made from two lumped junctions, we seek the maximum supercurrent $i_{\rm max}$ that can be put through the junction because for $i \leq i_{\rm max}$ only supercurrents flow through the junction. The maximum supercurrent that can be sent though the junctions occurs when $\sin \varphi(0) = \pm 1$, so that

$$i_{\max}(\Phi_J) = I_c \left| \frac{\sin \frac{\pi \Phi_J}{\Phi_o}}{\frac{\pi \Phi_J}{\Phi_o}} \right|$$
 (8.103)

Figure 8.15 shows $i_{\text{max}}(\Phi_J)$ and is referred to as the single junction interference pattern.

To understand why the maximum supercurrent has the general shape of Figure 8.15 we consider the current density distribution for different amounts of flux Φ_J in the junction, as shown in Figure 8.16. When the applied magnetic flux density B_o is zero, the flux through the junction Φ_J vanishes. Therefore, the gauge-invariant phase difference is a constant $\varphi(0)$ according to Equation 8.99. The resulting supercurrent density is constant throughout the junction so that the maximum supercurrent occurs when J_s is also a maximum, which happens when $\varphi(0) = \pi/2$. In Figure 8.16 the arrows are drawn proportional to the magnitude of supercurrent density $J_s(z)$ at a point z in the insulator when the current is a maximum; the direction of the arrows indicate the direction of the current density. The case of zero flux is shown in Figure 8.16a where the current density is a constant J_c . Also noted in Figure 8.16 is the value of the flux in the junction, the variation of the phase with z, the difference in the phase across the length d of the junction, and $\varphi(0)$ for the maximum current. If current less than the maximum were to be sent through the junction, then Figure 8.16a would look the same except that the arrows representing the magnitude of $J_s(z)$ would be scaled to $J_c \sin \varphi(0)$.

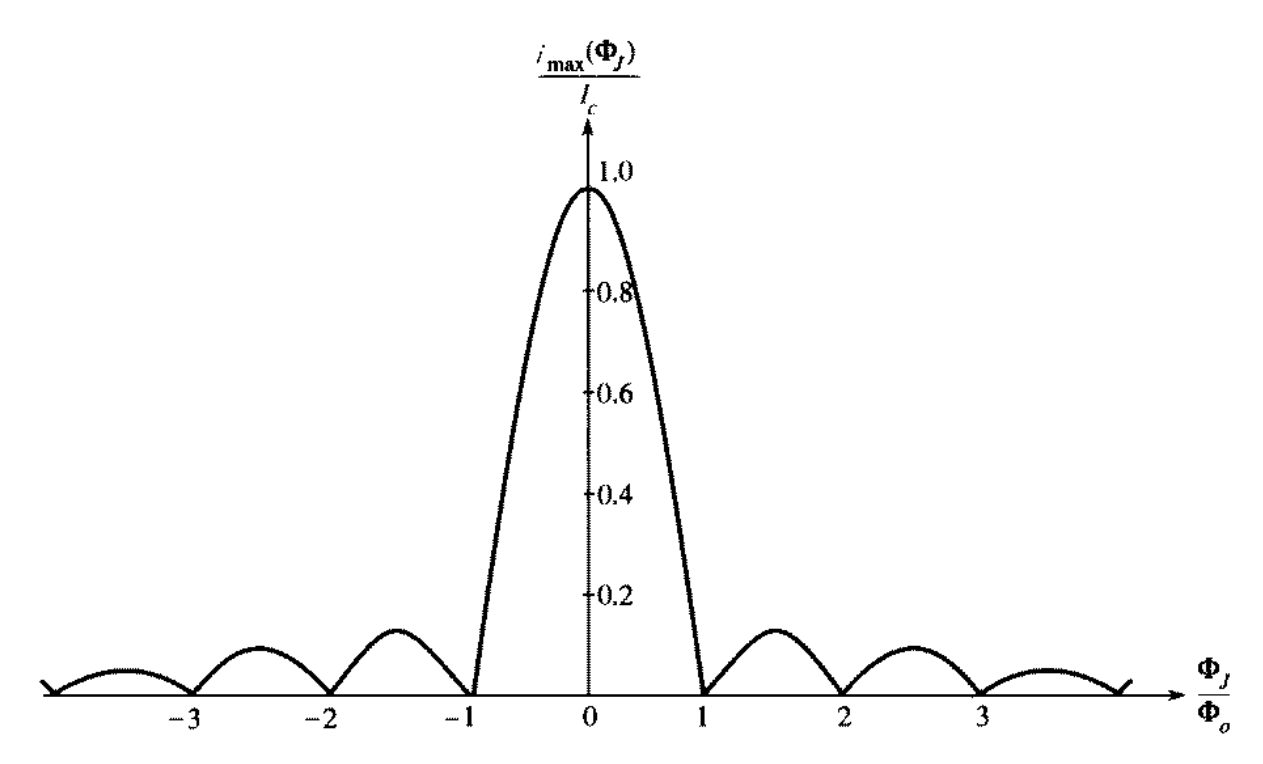


Figure 8.15 $i_{max}(\Phi_J)$ for a single short Josephson junction when the self-fields have been neglected.

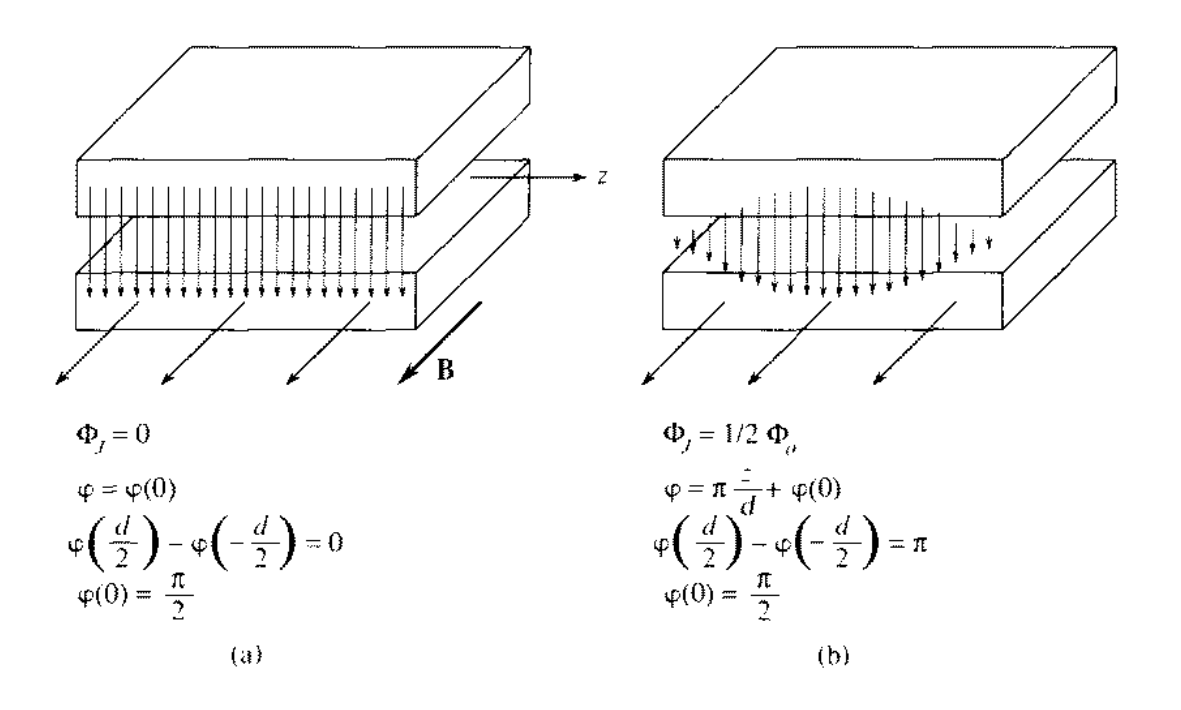
Now let the externally applied flux density be increased until $\Phi_J = \Phi_o/2$. Then $\varphi(z)$ varies linearly with z as

$$\varphi(z) = \frac{2\pi\Phi_J}{\Phi_o} \frac{z}{d} + \varphi(0) = \pi \frac{z}{d} + \varphi(0)$$
 (8.104)

according to Equation 8.99, as indicated in Figure 8.16b. Therefore, the supercurrent density varies sinusoidally with z. The difference between the phases from one end of the junction to the other is

$$\varphi\left(\frac{d}{2}\right) - \varphi\left(-\frac{d}{2}\right) = \pi, \qquad (8.105)$$

so that a half a period fits into the junction. Figure 8.16b shows the sinusoidal nature of the current density where the arrows indicate the direction and magnitude of the supercurrent in the junction. Which half period to put into the junction depends on the choice of $\varphi(0)$. In Figure 8.16b the phase was chosen to be $\varphi(0) = \pi/2$ so as to depict the maximum supercurrent density. The maximum total current must be more when there is no flux, in agreement with Equation 8.103. There are other possible choices of how to position the half period, which correspond to choosing different values of $\varphi(0)$. For example, if the period were moved to the left by a quarter period by choosing $\varphi(0) = 0$, then the supercurrent would be equal and opposite in the different halves of the junction so that the total current would be zero; this would clearly not be



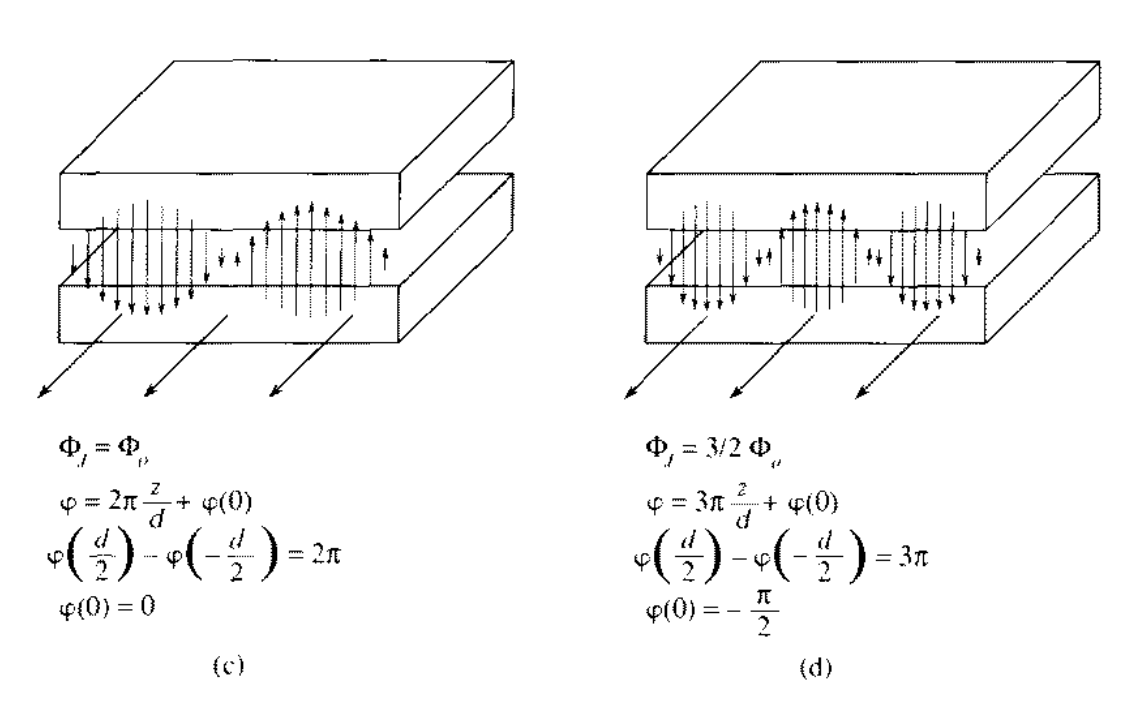


Figure 8.16 The current density distribution for $i_{\max}(\Phi_J)$ for a single short Josephson junction. The value of $\varphi(0)$ that maximizes the current density is chosen for each picture. Source: From D. N. Langenberg, D. J. Scalapino, and B. N. Taylor, "The Josephson Effects." Copyright © 1966 by Scientific American, Inc. All rights reserved. Reprinted with permission.

the scenario for the maximum current. Recall that it is only the supercurrent in the insulator that is shown in the figure. The supercurrent density is being driven from the top electrode to the bottom one. It is uniform upon entering the top electrode at $x = a + b_1$ because the length and the width were chosen smaller than the penetration depths. Nevertheless, to conform to the supercurrent density shown in the figure at the insulator, the supercurrent density must rearrange itself. This can be done because $b_1 \gg \lambda_1$. Likewise, the supercurrent density must rearrange itself to be uniform at $x = -(a + b_2)$, which it can also do because $b_2 \gg \lambda_2$.

When $\Phi_I = \Phi_o$, the total phase difference across the length of the junction is 2π so that a complete period fits in the junction, as shown in Figure 8.16c. The total current flowing through the junction is zero. If the position of the starting part of the period is changed by choosing a different $\varphi(0)$, a total period will still fit in. Yet for the choice $\varphi(0) = 0$ shown in Figure 8.16c, the supercurrent in the insulator must flow downward on the left side of the junction and upward on the right. How can the supercurrent density have such a pattern in the insulator and still have no net driving current so that the supercurrent density is zero at $x = a + b_1$ and $x = -(a + b_2)$? It can do so by having the pattern shown in Figure 8.17. The supercurrent on the left side of the junction turns around in the top electrode so as to match the supercurrent density in the insulator on the right side. The supercurrent can easily bend as needed since $b_1 \gg \lambda_1$. The resulting supercurrent density pattern in the superconductor resembles the pattern of a vortex, and is known as a Josephson vortex. But this vortex has no need of a normal core since the supercurrent density is zero in the center.

When $\Phi_J = 3\Phi_o/2$, then one and a half periods fit into the junction, as shown in Figure 8.16d. The current from the full period (a vortex) is zero so that the total current is determined by a half period. This current is smaller than

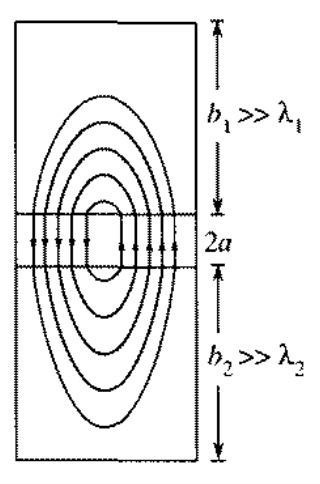


Figure 8.17 The supercurrent density distribution in the superconducting electrodes and across the insulator for the case of $\Phi_J = \Phi_o$. The pattern is known as a Josephson vortex.

when one half period fits the whole junction. Consequently, the current density will generally tend to decrease as Φ_J increases as shown in Figure 8.15.

As Φ_J increases further the supercurrent will be zero whenever an integral number n of Φ_o fit into the junction. This means that n complete periods are put into the junction corresponding to n complete vortices. Hence, we see that the driving current is zero whenever a full number of periods (that is, vortices) fit in the junction.

Josephson vortices are useful in understanding the interference pattern given by Equation 8.103 and depicted in Figure 8.15. Another useful method is the following analogy. Using Equations 8.100 and 8.101, we can write the current as

$$i = w \operatorname{Im} \left\{ e^{j\varphi(0)} \int_{-\infty}^{\infty} J_c(z) e^{jkz} dz \right\}, \qquad (8.106)$$

where $k = \frac{2\pi}{\Phi_o} B_o h_{\text{eff}}$. In general the integral in Equation 8.106 will be a complex number having both a magnitude and a phase. When the integral is multiplied by $e^{j\varphi(0)}$ only the phase of the resulting expression changes. Therefore, the maximum current is just the magnitude of the integral; namely,

$$i_{\max} = w \left| \int_{-\infty}^{\infty} J_c(z) e^{jkz} dz \right|. \tag{8.107}$$

Inspection of this equation shows that the maximum amount of the current is just the magnitude of the Fourier transform of the shape of the junction. This is analogous to the result in Fourier optics, which states that the intensity of the light is the Fourier transform of the slits. Here the Fourier transform variable is $k = \frac{2\pi}{\Phi_o} B_o h_{\text{eff}}$. For example, if the junction is a segment of length d, then its Fourier transform is a function of the form $\sin(kd/2)/(kd/2)$ in agreement with Equation 8.103. Likewise, if the configuration is two lumped junctions connected in parallel as in Figure 8.8, then the shape can be modeled as two impulse functions. This shape has the Fourier transform of the form $\cos(kd/2)$, which agrees with Equation 8.78.

Having found the interference pattern due to the short junction, we now find the energy W_J associated with a short Josephson junction, as shown in Figure 8.14. The energy W_J is

$$W_{J} = W_{s} + W_{in}, (8.108)$$

where W_s is the energy stored in the superconductor and W_{in} is the energy stored in the insulating region. For an MQS system W_s was found in Section 3.5 to be

$$W_s = \frac{1}{2\mu_o} \int_{V_s} \left(\mathbf{B}^2 + \mu_o \Lambda \mathbf{J}^2 \right) dv, \qquad (8.109)$$

where the integration is over the superconducting volume V_s and it is implicit that the current in this expression is the supercurrent only. This expression

is not valid for the insulating region because W_s was derived assuming the first London equation, which is not valid in the insulating region. Therefore, to find W_{in} we must return to the expression for the power delivered to the insulating region; namely, for an MQS system

$$\frac{d}{dt}W_{\rm in} = \int_{V_{\rm in}} \left(\mathbf{H} \cdot \frac{\partial \mathbf{B}}{\partial t} + \mathbf{E} \cdot \mathbf{J} \right) dv, \qquad (8.110)$$

where $V_{\rm in}$ is the volume of the insulating region. The second term in the integral can be simplified by using the current-phase relation (Equation 8.28). Note that the supercurrent J_s in Figure 8.14 is along the negative x-direction. Therefore,

$$\mathbf{J} = J_x(y, z) \, \mathbf{i}_x = -J_s(y, z) \, \mathbf{i}_x, \qquad (8.111)$$

and with Equation 8.100, we find that $\mathbf{J} = -J_c(y, z, t)\sin\varphi(y, z, t)\mathbf{i}_x$. The electric field is in the negative x-direction for the sign of the voltage chosen in Figure 8.14. If we assume that the insulator is thin enough so that the electric field is constant over it, then the voltage-phase relation (Equation 8.33) gives

$$E_x = -\frac{\Phi_o}{2\pi} \frac{1}{2a} \frac{\partial}{\partial t} \varphi(y, z, t), \qquad (8.112)$$

where the path of integration for E_x was taken directly across the insulator. With $\mathbf{B} = \mu_o \mathbf{H}$ and J_x and E_x , the power becomes

$$\frac{d}{dt}W_{\rm in} = \frac{d}{dt}\int_{V_{\rm in}} \left(\frac{1}{2\mu_o}\mathbf{B}^2 - \frac{\Phi_o}{2\pi}\frac{J_c}{2a}\cos\varphi\right)dv. \tag{8.113}$$

The energy in the insulating region is then

$$W_{\rm in} = \int_{V_{\rm in}} \left(\frac{1}{2\mu_o} \mathbf{B}^2 - \frac{\Phi_o}{2\pi} \frac{J_c}{2a} \cos \varphi \right) d\nu + W_o , \qquad (8.114)$$

where W_o is an integration constant. Since φ and J_c do not depend on x, the second term in W_{in} can be integrated over the height 2a of the insulator to give

$$W_{\rm in} = \frac{1}{2\mu_o} \int_{V_-} \mathbf{B}^2 dv - \int_{S_-} \frac{\Phi_o}{2\pi} J_c(y, z) \cos \varphi(y, z, t) \, dy \, dz + W_o$$
, (8.115)

where S_{in} is the surface area of the insulator. Thus the total energy is

$$W = \frac{1}{2\mu_o} \int_{V_s + V_{tn}} \mathbf{B}^2 dv + \frac{1}{2} \int_{V_s} \Lambda \mathbf{J}^2 dv + \int_{S_{tn}} \frac{\Phi_o}{2\pi} J_c(y, z) \left[1 - \cos \varphi(y, z, t) \right] dy dz.$$
 (8.116)

In the last term the constant W_o was chosen as

$$W_o = \int_{S_{in}} \frac{\Phi_o}{2\pi} J_c(y, z) \, dy \, dz = \frac{I_c \Phi_o}{2\pi}, \qquad (8.117)$$

so that the energy would conveniently match that of the lumped junction (Equation 8.41) whose critical current can be modeled as $J_c = I_c \delta(y) \delta(z)$.

We are now in a position to put our definition of a short junction on a more well defined basis. The assumption that in a short junction one is able to disregard the magnetic field produced by the currents is now more naturally interpreted as the condition that the energy stored in the junction due to the external field W_B is much larger than the energy due to the currents that flow W_J . In other words, a short junction is one in which $W_B \gg W_J$. Now W_B is just the first two integrals in Equation 8.116. For the case where the thicknesses of the superconductors are larger than the penetration depths, the first integral dominates the energy so that

$$W_B = \frac{1}{2\mu_o} \int_{V_z + V_{in}} \mathbf{B}^2 \, dx \, dy \, dz \,. \tag{8.118}$$

The region of integration over which the magnetic field affects the junction is the cross-sectional area wd times the effective distance h_{eff} the magnetic field penetrates, since the magnetic field penetrates not only the thickness of the insulator but also a λ into each superconducting electrode. Consequently,

$$W_B = \frac{1}{2\mu_o} B_o^2 h_{\text{eff}} w d = \frac{1}{2\mu_o} \frac{\Phi_J^2 w}{h_{\text{eff}} d}$$
 (8.119)

Now the energy due to the currents in the junction W_J is just the last integral in Equation 8.116 so that

$$W_J = \frac{\Phi_o}{2\pi} \int_{-w/2}^{w/2} \int_{-d/2}^{d/2} dy \, dz \, J_c(y, z) \left[1 - \cos \varphi(z) \right] \,. \tag{8.120}$$

For simplicity we will consider the case of a constant critical current density J_c . Using Equation 8.99 in integrating Equation 8.120, we find that

$$W_{J} = \frac{\Phi_{o}I_{c}}{2\pi} \left(1 - \frac{\sin\frac{\pi\Phi_{J}}{\Phi_{o}}}{\frac{\pi\Phi_{J}}{\Phi_{o}}} \cos\left(\varphi(0)\right) \right) . \tag{8.121}$$

We have used again that $\Phi_J = B_o h_{\text{eff}} d$ is the flux through the junction and $I_c = J_c w d$ is the maximum critical current through the junction.

A typical flux Φ_J for the short junction approximation is Φ_o ; this is also

the flux for which the identifiable structure of a vortex appears. With $\Phi_J = \Phi_o$ in Equation 8.121,

$$W_J = \frac{\Phi_o I_c}{2\pi} \,. \tag{8.122}$$

The contribution from the external field is

$$W_B = \frac{\Phi_o^2 w}{2\mu_o h_{\text{eff}} d} \,. \tag{8.123}$$

The condition for our analysis for a short junction to be accurate is that

$$\frac{\Phi_o I_c}{2\pi} \ll \frac{\Phi_o^2 w}{2\mu_o h_{\text{eff}} d} \,. \tag{8.124}$$

Writing the critical current in terms of the critical current density, we can cast this inequality into an equivalent expression in terms of the length of the junction; namely,

$$d \ll \ell_J \,, \tag{8.125}$$

where ℓ_J is a characteristic length of the Josephson junction and is given by

$$\ell_J = \sqrt{\frac{\pi \Phi_o}{\mu_o J_c h_{\text{eff}}}} \,. \tag{8.126}$$

Hence, a short junction is one whose length is smaller than ℓ_J . In Section 8.6 we see how ℓ_J enters in as the natural length scale in the equations that describe extended junctions.

Having seen that vortices can be used to visualize the current distribution for a current driven junction, we now show that these same vortices can be used to understand properties of short junctions when they are driven by a voltage source. Let a constant voltage V_o be applied across the junction. For a short junction the flux density is approximately equal to the external field in the y-direction so that $B \approx B_o$. Hence, the gauge-invariant phase difference must satisfy both Equation 8.96,

$$\frac{\partial \varphi}{\partial z} = \frac{2\pi}{\Phi_o} B_o h_{\text{eff}}, \tag{8.127}$$

and the Josephson voltage-phase relation Equation 8.33,

$$\frac{\partial \varphi}{\partial t} = \frac{2\pi}{\Phi_o} V_o. \tag{8.128}$$

The solution to these equations is

$$\varphi(z,t) = \frac{2\pi}{\Phi_o} B_o h_{\text{eff}} z + \frac{2\pi}{\Phi_o} V_o t + \varphi(0)$$
 (8.129)

$$=\frac{2\pi}{\Phi_o}B_oh_{\text{eff}}(z-ut)+\varphi(0), \qquad (8.130)$$

where

$$u = -\frac{V_o}{B_o h_{\text{eff}}}.$$
 (8.131)

The current density is then dependent on both space and time as

$$J(y,z,t) = J_c(y,z)\sin\varphi(z-ut). \tag{8.132}$$

The current through the junction has the same spatial pattern as for a zero-voltage case but the pattern itself moves with velocity u. For the case of a constant J_c , the patterns are the ones depicted in Figure 8.16. These patterns can be pictured as a vortex with a period $p = \Phi_o d/\Phi_{\rm ext}$; this is the length over which the phase changes by 2π along the z-direction. As defined, the period p can be larger or smaller than the length of the junction. Let n_v be the number (or fraction) of vortices in the junction at some time. Therefore,

$$n_{\nu} = \frac{d}{p} = \frac{\Phi_{\text{ext}}}{\Phi_o}. \tag{8.133}$$

Then the amount $\Delta \varphi$ that the gauge-invariant phase difference changes in the junction is just

$$\Delta \varphi = 2\pi \mathbf{n}_{\nu} . \tag{8.134}$$

Consequently, the rate at which vortices move through the junction is

$$\frac{d}{dt}\mathbf{n}_{v} = \frac{1}{2\pi}\frac{d\Delta\varphi}{dt} = \frac{V_{o}}{\Phi_{o}}.$$
 (8.135)

This is the same relationship that was found in Section 7.4 for flux flow for vortices in a type II superconductor. However, note that vortices in a Josephson junction do not have a normal core but still dissipate energy when they move.

8.6 LONG JOSEPHSON JUNCTIONS

We now consider the effects of the self-induced magnetic fields on the behavior of the extended Josephson junction shown in Figure 8.14. The derivation leading to the spatial change of the gauge-invariant phase difference due to the magnetic

flux density in Equation 8.96 is general for the geometry considered, so again we have

$$\frac{\partial \varphi}{\partial z} = \frac{2\pi}{\Phi_o} B_y h_{\text{eff}} \,, \tag{8.136}$$

where $h_{\text{eff}} = \lambda_1 + \lambda_2 + 2a$. The magnetic field is produced by both the applied field and the currents and must satisfy Ampère's law with the constitutive relationships $\mathbf{B} = \mu_o \mathbf{H}$ and $\mathbf{D} = \epsilon \mathbf{E}$ in the insulator:

$$\nabla \times \mathbf{B} = \mu_o \mathbf{J} + \epsilon \mu_o \frac{\partial \mathbf{E}}{\partial t} \,. \tag{8.137}$$

We first consider the case where the fields and currents do not depend on time. The externally applied magnetic field is in the y-direction. The resulting magnetic field depends only on z, because d and w are both much greater than 2a. Therefore effects on the fields due to the edges of the junction are negligible. Likewise, the current density in the insulator is in the negative x-direction and also depends only on z.

Ampère's law gives

$$\frac{\partial B_{y}(z)}{\partial z} = -\mu_{o} J_{x}(z) . \tag{8.138}$$

The spatial derivative of Equation 8.136 combined with Equation 8.138 gives

$$\frac{\partial^2 \varphi(z)}{\partial z^2} = -\frac{2\pi \mu_o h_{\text{eff}}}{\Phi_o} J_x(z). \qquad (8.139)$$

We further assume that the critical current density is a constant J_c over the area of the junction. However, note again that the supercurrent in Figure 8.14 is along the negative x-direction. Therefore, as in Equation 8.111, $J_x(y,z) = -J_s(y,z)$ so that $J_x(z) = -J_c \sin \varphi(z)$. Equation 8.139 can then be written as

$$\frac{\partial^2 \varphi(z)}{\partial z^2} = \frac{\sin \varphi(z)}{\lambda_I^2} \,. \tag{8.140}$$

Here λ_J is known as the *Josephson penetration depth* and is given by

$$\lambda_J = \sqrt{\frac{\Phi_o}{2\pi\mu_o J_c h_{\text{eff}}}} . \tag{8.141}$$

Note that within a factor of order unity, λ_J is equal to the characteristic length ℓ_J found in Section 8.5 (Equation 8.126).

Hence, we see that the gauge-invariant phase difference satisfies the nonlinear differential equation 8.140, which in most cases must be solved numerically.

We will solve the nonlinear equation in a few special cases where analytical solutions exists to get a feeling for the types of solutions.

The first case where an approximate solution to Equation 8.140 can be given is when the length of the junction in the z-direction d is much smaller than the Josephson penetration depth, that is, when $d \ll \lambda_J$, which is just the condition for a short junction. Equation 8.140 can then be approximated as $\partial^2 \varphi(z)/\partial z^2 \approx 0$, which has the solution $\partial \varphi/\partial z$ is a constant. Comparing this solution with Equation 8.96, we find that the condition for a short junction is equivalent to the assumption of neglecting the self-fields, as was done in the previous Section 8.5. Consequently, the solution for the phase is given by Equation 8.99. To get an estimate of typical Josephson penetration depths let $h_{\rm eff} \approx 500$ nm, then $\lambda_J \approx 2 \, \mu {\rm m}$ for $J_c = 10^8 \, {\rm A/m^2}$, and $\lambda_J \approx 20 \, \mu {\rm m}$ for $J_c = 10^6 \, {\rm A/m^2}$.

Another solution to Equation 8.140 is the particular solution to the differential equation; namely,

$$\varphi(z) = -2\sin^{-1}\left(\operatorname{sech}\frac{z - z_o}{\lambda_J}\right), \qquad (8.142)$$

which can be verified by direct substitution. Here z_o is a constant. The corresponding magnetic field is found from Equation 8.136 and is

$$B_{y}(z) = \frac{\Phi_{o}}{\pi \lambda_{J} h_{\text{eff}}} \operatorname{sech}\left(\frac{z - z_{o}}{\lambda_{J}}\right)$$
 (8.143)

Likewise, the resulting current density is found from Equation 8.138 and is

$$J_x(z) = \frac{\Phi_o}{\pi \mu_o \lambda_J^2 h_{\text{eff}}} \tanh\left(\frac{z - z_o}{\lambda_J}\right) \operatorname{sech}\left(\frac{z - z_o}{\lambda_J}\right)$$
 (8.144)

$$=2J_c \tanh\left(\frac{z-z_o}{\lambda_J}\right) \operatorname{sech}\left(\frac{z-z_o}{\lambda_J}\right) . \tag{8.145}$$

For the general solution to a differential equation, we must also know not only the particular solutions but also the homogeneous solutions in order to match the boundary conditions. We will, however, restrict ourselves to those special cases where only the particular solution given by Equations 8.142–8.145 is needed.

One example is to consider the case where the origin is chosen at z_o and $\varphi(z)$ is chosen to vanish at $z=\pm\infty$ in a junction of infinite length. Then the particular solution is the full solution that satisfies the boundary conditions and the magnetic field and current density are shown in Figure 8.18. For this particular solution the field and current density decay with the characteristic length of λ_J . Furthermore, the current density does not have a maximum at the same position where the magnetic field is largest. To understand what this particular solution corresponds to physically we note that the total current in

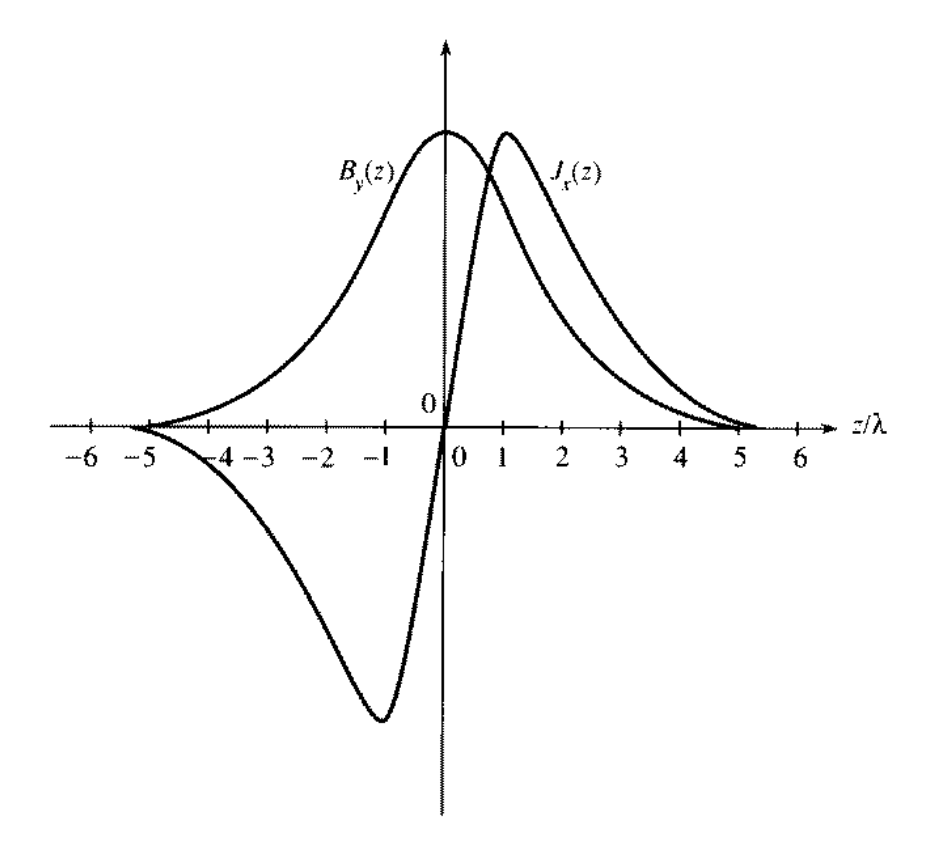


Figure 8.18 $B_y(z)$ and $J_x(z)$ for a vortex solution in a long Josephson junction when the self-fields have been included.

the junction is zero and the total flux integrates to Φ_o . Hence, we have the case similar to the situation in Figure 8.16c so that we interpret this special solution as a Josephson vortex in a long junction. Therefore, we find that the Josephson vortex is mostly confined to a length of the order of λ_I .

Another example that is solved by the particular solution is shown in Figure 8.19 and is known as the asymmetrical in-line Josephson junction. A surface

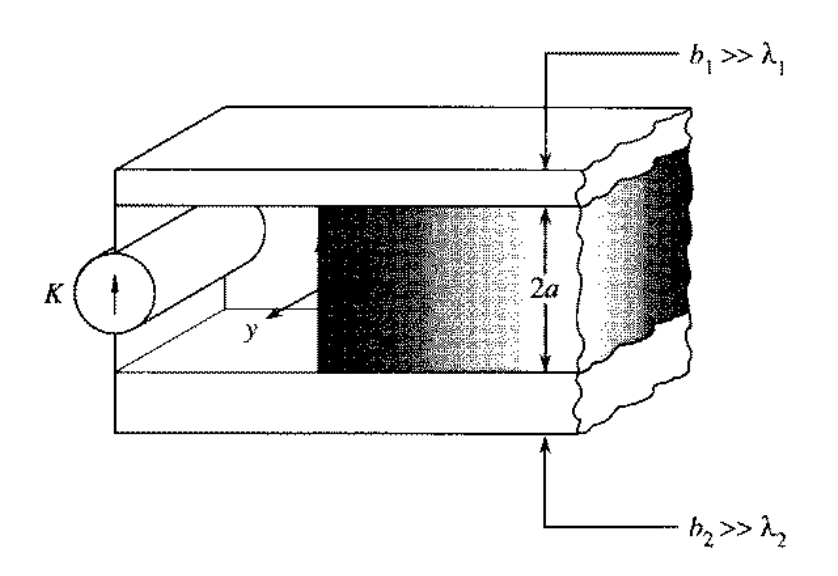


Figure 8.19 An Asymmetrical In-Line Josephson Junction

current density K is driven through the two superconducting electrodes, which have thicknesses larger than their respective penetration depths λ_1 and λ_2 . The insulating barrier is semiinfinite and exists for $z \ge 0$. The current must pass though the insulating barrier as a Josephson current. Again the dependence of the fields and current density in the insulator varies only in the z-direction. In the empty space between the superconducting planes for $z \le 0$, $B_y(z) = \mu_o K$. In the region $z \ge 0$, the gauge-invariant phase difference is governed by Equation 8.142, and the fields and currents are given by Equations 8.143 and 8.145. The constant z_o is found by demanding that the tangential component of the field be continuous; therefore, z_o is such that

$$B_{y}(0) = \mu_{o}K = \frac{\Phi_{o}}{\pi \lambda_{J} h_{\text{eff}}} \operatorname{sech}\left(\frac{z_{o}}{\lambda_{J}}\right)$$
 (8.146)

We can rewrite Equations 8.143-8.146 for the current density and fields for z > 0 as

$$B_{y}(z) = \mu_{o}K \frac{\operatorname{sech}\left(\frac{z-z_{o}}{\lambda_{J}}\right)}{\operatorname{sech}\left(\frac{z_{o}}{\lambda_{J}}\right)}$$
 (8.147)

and

$$J_{x}(z) = \frac{K}{\lambda_{J}} \frac{\tanh\left(\frac{z - z_{o}}{\lambda_{J}}\right) \operatorname{sech}\left(\frac{z - z_{o}}{\lambda_{J}}\right)}{\operatorname{sech}\left(\frac{z_{o}}{\lambda_{J}}\right)},$$
(8.148)

where

$$z_o = \lambda_J \operatorname{sech}^{-1} \left(\frac{K}{2\lambda_J J_c} \right) . \tag{8.149}$$

The maximum surface current density K_{max} that can be driven through this in-line junction occurs when $z_o = 0$, so that $K_{\text{max}} = 2\lambda_J J_c$. This result is reasonable since the maximum surface current density is on the order of $J_c \lambda_J$.

As with a short junction, an energy W can be found for long Josephson junctions. In fact the analysis in Section 8.5 leading the expression for W in Equation 8.116 also holds for the long junction. The total energy is then the sum of the energy in the insulating region W_{in} and the energy of the superconducting region W_s . Recall that

$$W_s = rac{1}{2\mu_o} \int_{\mathcal{V}} \left(\mathbf{B}^2 + \mu_o \Lambda \mathbf{J}^2 \right) dv \,,$$
 (8.150)

from Equation 8.109 and

$$W_{\rm in} = \frac{1}{2\mu_o} \int_{V_{\rm in}} \mathbf{B}^2 dv + \int_{S_{\rm in}} \frac{\Phi_o}{2\pi} J_c(y, z) \left[1 - \cos \varphi(y, z, t) \right] dy dz, \qquad (8.151)$$

from Equations 8.115 and 8.117. Expressing the magnetic flux intensity in terms of the gauge-invariant phase difference with Equation 8.136 and integrating over x and y results in

$$W_{\rm in} = \frac{\Phi_o J_c w}{2\pi} \int dz \left[\frac{1}{2} \lambda_J^2 \left(\frac{\partial \varphi}{\partial z} \right)^2 + (1 - \cos \varphi) \right] . \tag{8.152}$$

As an example we calculate the energy stored in the vortex solution of Equation 8.142. We use a trigonometric identity and Equation 8.142 to write the second term in the integral as

$$1 - \cos \varphi = 2 \sin^2 \left(\frac{\varphi}{2}\right) = 2 \operatorname{sech}^2 \left(\frac{z}{\lambda_J}\right). \tag{8.153}$$

Likewise, the first term in the integral can be simplified by using Equations 8.143 and 8.136 to give

$$\frac{1}{2}\lambda_J^2 \left(\frac{\partial \varphi}{\partial z}\right)^2 = 2 \operatorname{sech}^2 \left(\frac{z}{\lambda_J}\right). \tag{8.154}$$

Therefore, the energy per unit length of the vortex, $\mathcal{E}_{\mathcal{V}}$, is

$$\mathcal{E}_{V} = \frac{W_{\rm in}}{w} = \frac{2\Phi_{o}J_{c}}{\pi} \int_{-\infty}^{\infty} dz \, \operatorname{sech}^{2}\left(\frac{z}{\lambda_{J}}\right) = \frac{4\Phi_{o}J_{c}\lambda_{J}}{\pi}. \tag{8.155}$$

In the presence of a magnetic field we find that the magnetic field intensity B_{c1} at which the vortex will first go into the junction is given by a similar argument in Section 6.5 for when flux first goes into a type II superconductor; namely,

$$B_{c1} = \frac{\mu_o \mathcal{E}_V}{\Phi_o}. \tag{8.156}$$

Hence,

$$B_{c1} = \frac{4\mu_o J_c \lambda_J}{\pi} = \frac{2\Phi_o}{\pi^2 \lambda_J h_{\text{eff}}}.$$
 (8.157)

This result is intuitive because it is approximately the magnetic field intensity for a flux quantum area distributed over an area λ_I by h_{eff} .

Just as in the case with the short junction, vortices can also be used to visualize the current distribution of long junctions that are driven by a voltage

source. The gradient of the gauge-invariant phase difference is given by Equation 8.136 with the magnetic field intensity being both a function of z and t. The partial derivative with respect to z of Equation 8.136 when combined with Ampère's law from Equation 8.137 gives

$$\frac{\partial^2 \varphi(z,t)}{\partial z^2} = -\frac{2\pi h_{\text{eff}}}{\Phi_o} \left[\mu_o J_x(z,t) + \mu_o \epsilon \frac{\partial E_x}{\partial t} \right] . \tag{8.158}$$

The parallel plate structure of the junction allows us to write the electric field as $E_x = -v/2a$, where v is the voltage across the junction, the path of integration of E is taken directly across the junction, and fringing fields have been neglected. Substituting for E_x and using Equations 8.111, 8.28, and 8.33, we see that

$$\frac{\partial^2 \varphi}{\partial z^2} = \frac{2\pi h_{\text{eff}}}{\Phi_o} \left[\mu_o J_c \sin \varphi + \frac{\epsilon \mu_o \Phi_o}{2\pi (2a)} \frac{\partial^2 \varphi}{\partial t^2} \right] . \tag{8.159}$$

Using the definition of the Josephson penetration depth from Equation 8.141, we can rearrange Equation 8.159 to write a wave equation for the junction as

$$\frac{\partial^2 \varphi}{\partial z^2} - \frac{1}{u_p^2} \frac{\partial^2 \varphi}{\partial t^2} = \frac{1}{\lambda_J^2} \sin \varphi \,, \tag{8.160}$$

where u_p is the velocity of the TEM mode in a transmission line and is given by

$$u_p = \sqrt{\frac{2a}{\mu_o \epsilon h_{\text{eff}}}} = \frac{1}{\sqrt{\mu_o \epsilon}} \sqrt{\frac{a}{\lambda + a}}$$
 (8.161)

Equation 8.160 is known as the sine-Gordon equation. It is nonlinear and has many interesting types of behavior. We give only a small sampling of some of the solutions. One familiar solution occurs when the critical current is zero. In this case the right-hand side of Equation 8.160 vanishes and reduces to the familiar linear wave equation. In fact by taking the partial time derivative of the linear wave equation and recalling that the voltage is proportional to the time derivative of the phase, we find the usual wave equation for the voltage for the TEM mode for the parallel plate geometry discussed in Section 4.4.

Another class of solutions can be studied by linearizing the sine-Gordon equation. Let

$$\varphi(z,t) = \varphi_o(z) + \varphi_1(z,t), \qquad (8.162)$$

where $\varphi_o(z)$ is a time independent solution and φ_1 is a small deviation from $\varphi_o(z)$ such that $\varphi_1 \ll \varphi_o(z)$. Under these conditions a good approximation is

$$\sin \varphi(z,t) \approx \sin \varphi_o + \varphi_1 \cos \varphi_o$$
. (8.163)

Substituting Equations 8.162 and 8.163 into Equation 8.160 and keeping only the linear terms in φ_1 we find that

$$\frac{\partial^2 \varphi_o}{\partial z^2} + \frac{\partial^2 \varphi_1(z,t)}{\partial z^2} - \frac{1}{u_p^2} \frac{\partial^2 \varphi_1(z,t)}{\partial t^2} = \frac{\sin \varphi_o}{\lambda_J^2} + \frac{\cos \varphi_o}{\lambda_J^2} \varphi_1(z,t). \quad (8.164)$$

The first term on the left-hand side of Equation 8.164 cancels with the first term on the right-hand side because φ_o satisfies the time independent equation. Therefore,

$$\frac{\partial^2 \varphi_1(z,t)}{\partial z^2} - \frac{1}{u_p^2} \frac{\partial^2 \varphi_1(z,t)}{\partial t^2} = \frac{\cos \varphi_o}{\lambda_J^2} \varphi_1(z,t). \tag{8.165}$$

If we further assume that φ_o varies slowly over the scale that φ_1 changes, then φ_o can be considered a constant. In such a case the solution is

$$\varphi_1(z,t) = e^{-j(kz-\omega t)}, \qquad (8.166)$$

and ω satisfies the dispersion relationship

$$\omega^2 = u_p^2 k^2 + \omega_{p,J}^2 \,. \tag{8.167}$$

Here $\omega_{p,J}$ is the Josephson plasma frequency and is given by

$$\omega_{p,J}^2 = \frac{u_p^2}{\lambda_J^2} \cos \varphi_o . \qquad (8.168)$$

For frequencies below $\omega_{p,J}$, k is imaginary so that no propagating solutions exists for these low frequencies. For frequencies greater than $\omega_{p,J}$ modes will propagate, and, in particular, at $\omega_{p,J}$ the wavelength is infinitely long just as it is for the plasma frequency in a metal. Typical parameters for Nb Josephson junctions imply $\omega_{p,J}$ of a few gigahertz when $\varphi_o \approx 0$.

8.7 SUMMARY

In this chapter we have shown how the macroscopic wavefunction can extend across the insulating barrier of a tunnel junction and allow a supercurrent to flow across the insulator. The resulting Josephson current is maintained by a difference in the quantum mechanical phase across the junction. We found that the supercurrent density through the tunnel junction varies sinusoidally with the difference in the gauge-invariant phase difference across the junction and has a maximum value known as the critical current density J_c . Throughout this chapter we have considered only basic Josephson junctions where the current densities are always less than J_c so that the current is always a supercurrent.

8.7 Summary 439

For a junction that is considered a lumped element, the Josephson current i across the junction is related to the gauge-invariant phase difference φ by the current-phase relation of

$$i = I_c \sin \varphi$$
.

The gauge-invariant phase difference across the junction is given by

$$\varphi = \theta_1 - \theta_2 - \frac{2\pi}{\Phi_o} \int_1^2 \mathbf{A}(\mathbf{r}, t) \cdot d\mathbf{1},$$

where A is the magnetic vector potential and θ is the phase of the wavefunction. The numbered labels refer to the two sides of the junction. If the phase difference changes in time, then there is a voltage v across the junction that satisfies the voltage-phase relation

$$\frac{d\varphi}{dt} = \frac{2\pi}{\Phi_o} v .$$

These three equations govern the properties of basic lumped Josephson junctions.

The sinusoidal current-phase relation leads to a number of properties that are periodic. For example, the energy W_J of the junction is periodic in the gauge-invariant phase difference as

$$W_J = \frac{\Phi_o I_c}{2\pi} - \frac{\Phi_o I_c}{2\pi} \cos \varphi.$$

If a constant voltage is applied across the basic junction, then φ increases linearly in time. However, the sinusoidal current-phase relation means that a sinusoidal current in time then flows. Another example of the periodic phenomena that occur is the periodic response of a SQUID to an externally applied magnetic field. This periodic response is a result of φ depending on the applied field and enables the designing of a device that can sense flux to a fraction of a flux quantum Φ_{ϱ} .

For distributed junctions instead of lumped junctions, we saw how the current-phase and the current-voltage relations could be generalized by having the gauge-invariant phase difference and the current density depend on their position in the junction. Again these relations result in the same general types of periodic behavior as for a lumped junction. For example, a constant voltage still results in an alternating current. Moreover, we found that this alternating current is due to Josephson vortices moving across the junction. In an applied magnetic field a single distributed junction resembled a lumped junction in that its current is periodic in the applied magnetic field. Vortices again provided a way to understand this periodic behavior.

When considering the distributed junction, we found a characteristic length of the junction, λ_J , the Josephson penetration length that is given by

$$\lambda_J = \sqrt{rac{\Phi_o}{2\pi\mu_o J_c h_{
m eff}}} \; .$$

Here $h_{\rm eff}$ is the effective penetration depth into the junction. For short junctions whose characteristic length is smaller than λ_J , the magnetic field is the applied field. Conversely, for a long junction whose characteristic length is larger than λ_J , the self-fields generated by the currents had to be included in the magnetic field. This is analogous to including the self-inductance of a basic lumped junction SQUID.

References for Chapter 8

A derivation of the current-phase relation for the Josephson junction, similar to the one in this chapter, is given in "Macroscopic Quantum Phenomena in Superconductors" by R. de Bruyn Ouboter in Chapter 2 of Superconductor Applications: SQUIDs and Machines edited by B. B. Schwartz and S. Foner (Plenum, 1977). Another such development of the current-phase relation for the Josephson junction is given in Chapter 13 of Fundamentals of Solid State Physics by J. R. Christman (Wiley, 1988). This section (13.4) of the book is self-contained and can be read independently of the rest of the chapter. Most of the other elementary derivations of the current-phase relation are based on an argument that requires more familiarity with quantum mechanics than used in this book. Nevertheless, this argument is highly readable and is given in Chapter 21 in the The Feynman Lectures on Physics Volume III by R. P. Feynman, R. B. Leighton, and M. Sands (Addison-Wesley, 1965). An argument similar to the one given in this book but applied to structures other than a tunnel junction is given in "Superconducting Weak Links" by K. K. Likharev in Reviews of Modern Physics 51, 101 (1979). Although the article is at an advanced level, its introduction, which contains the argument, is at a more intermediate level.

Most of the discussions of lumped junctions include the resistance of the junction, which is not discussed in this book until the next chapter. Nevertheless, many of the examples given in these books discuss the limit in which the resistance can be neglected and hence is equivalent to the basic lumped junction. Chapter 5 of *Principles of Super-conductive Devices and Circuits* by T. Van Duzer and C. W. Turner (Elsevier, 1981) is devoted entirely to circuits based on lumped junctions. A concise treatment of some of the main features of lumped junctions is given in Chapter 5 of *Superfluidity and Superconductivity* by D. R. Tilley and J. Tilley (Hilger, 1986).

The SQUID with two parallel basic lumped junctions is discussed in depth in Section 5.10 of Van Duzer and Turner's book. The original work in this area is reviewed extensively in "Superconducting Point Contacts Weakly Connecting Two Superconductors" by R. de Bruyn Ouboter and A. Th. A. M. de Waele in Chapter 6 of *Progress in Low Temperature Physics*, volume VI edited by C. J. Gorter (North-Holland, 1970). Although ostensibly devoted to point contacts instead of tunnel junctions, the equations for the SQUID are identical for any device satisfying the Josephson current-phase relation. A briefer review is given by de Bruyn Ouboter in the book edited by Foner and

Schwartz. Chapter 14 in Superconductive Tunnelling and Applications by L. Solymar (Wiley, 1972) discusses not only a device containing two junctions in parallel but also a superconducting ring with one junction. A thorough treatment, including a discussion of the thermodynamic energies involved, of superconducting loops with basic lumped Josephson junctions is given in Chapter 12 of Physics and Applications of the Josephson Effect by A. Barone and G. Paterno (Wiley, 1982). This chapter also discusses some of the nonlinear dynamics that such loops can display.

A discussion of distributed junctions can be found in most of the books already cited, because distributed junctions are often discussed before lumped junctions. Chapter 4 of Van Duzer and Turner's book gives a discussion at the same level as this chapter. Vortices in short junctions are discussed with some excellent graphics in "The Josephson Effects" by D. N. Langenberg, D. J. Scalapino, and B. N. Taylor in Scientific American 214, No. 5, 30 (1966). Vortex solutions in a long junction are nicely developed in Chapter 12 of Solymar's book. A careful discussion of the gauge choice for the vector potential is given in Section 6.2 of Introduction to Superconductivity by M. Tinkham (Krieger, 1980). Most other books assume the London gauge when calculating the effects of the magnetic field on a single junction but this fact is rarely explicitly stated. Tinkham, however, works the problem in two different gauges. Not realizing which gauge is chosen accounts for most of the erroneous schemes for measuring the absolute value of the vector potential with Josephson junctions.

Problems

Problem 8.1 (Supercurrent Equation): Consider a Josephson junction consisting of identical superconductors so that $n_1^* = n_2^* = n_s^*$. Let the spacing between the two materials be a.

- a. In the absence of any vector potential, show that the Josephson current-phase relation given by Equation 8.18 reduces to the supercurrent equation (Equation 8.1) in the limit as the spacing a goes to zero such that the two separated superconductors become one continuous superconductor. Assume that J_c is given by Equation 8.19 and that the difference in phase $\theta_1 \theta_2$ becomes small as a goes to zero.
- b. Repeat part (a) with the vector potential included in the current-phase relation as in Equations 8.28 and 8.29.

Problem 8.2 (A Loop with a Single Junction): Consider a single lumped Josephson junction that is connected by a superconducting loop with inductance L.

a. If there are no applied magnetic fields, show that the current in the loop can take on values given by

$$I = -I_c \sin\left(\frac{2\pi LI}{\Phi_o}\right) .$$

Find the allowed values of I for $LI_c = 6\Phi_o$.

Show that the energy is given by

$$W = W_{bo} - \frac{\Phi_o I_c}{2\pi} \cos\left(\frac{2\pi LI}{\Phi_o}\right) + \frac{1}{2}LI^2.$$

Plot $W - W_{Io}$ versus I for $LI_c = 6\Phi_o$. Show that all the allowed values except I = 0 are metastable, that is, only I = 0 is the true minimum.

Problem 8.3: Now apply a magnetic flux Φ_{ext} to the configuration in Problem 8.2.

a. Show that the total flux Φ and the current I are given by

$$\Phi = \Phi_{\rm ext} - LI_c \sin\left(\frac{2\pi\Phi}{\Phi_o}\right)$$

and

$$I = -I_c \sin\left(\frac{2\pi\Phi}{\Phi_o}\right) .$$

b. For small inductances $L \approx 0$, show that the energy is approximately given by

$$W(I) = W_{lo} - \frac{\Phi_o I_c}{2\pi} \cos\left(\frac{2\pi\Phi_{\text{ext}}}{\Phi_o}\right)$$

and that

$$W(I) - W(I_c) = -\frac{\Phi_o I_c}{2\pi} \cos\left(\frac{2\pi\Phi_{\text{ext}}}{\Phi_o}\right).$$

c. When the inductance is large, the total flux is quantized so that

$$\Phi = \Phi_{\rm ext} + LI = n\Phi_a$$
.

Show that the energy is approximately given by

$$W(I) = \frac{1}{2L} (\Phi_{\rm ext} - n\Phi_o)^2$$

and that

$$W(I) - W(I_c) = \frac{1}{2L} (\Phi_{\text{ext}} - n\Phi_o)^2 - \frac{\Phi_o^2}{8\pi^2 L} \left(\frac{2\pi L I_c}{\Phi_o} + \frac{\pi}{2} \right)^2.$$

d. Plot Φ versus $\Phi_{\rm ext}$ and also $W(I)-W(I_c)$ versus $\Phi_{\rm ext}$ for the two limiting cases considered in parts (b) and (c). Note that when $W(I)-W(I_c)=0$ that the system will switch to the normal state, and will then be able to adjust the value of n to be in the lowest energy state as the externally applied flux is changed. The plot of Φ versus $\Phi_{\rm ext}$ will be hysteretic for part (c).

Problem 8.4 (Current Driven Junction): A single basic lumped junction with a critical current of I_c is driven by a current source

$$i(t) = I_0 + I_1 \cos \omega_1 t$$

as shown in Figure P8.1. The dc part of the current is given by I_o and the ac part is at a frequency of ω_s . The driving current i(t) is always less than the critical current, that is, $|I_o| + |I_s| < I_c$.

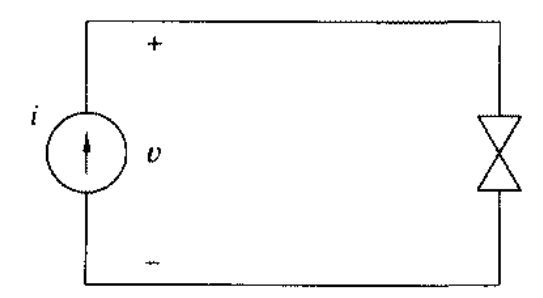


Figure P8.1 A Single Basic Lumped Junction Driven by a Current Source

a. For this circuit show that, in general, the phase is

$$\varphi(t) = \sin^{-1}\left(\frac{I_o + I_s\cos\omega_s t}{I_c}\right),\,$$

and the voltage across the junction is

$$v = \frac{\Phi_o}{2\pi} \frac{1}{\frac{\partial i}{\partial \varphi}} \frac{di}{dt} = -\frac{\Phi_o}{2\pi I_c} \frac{\omega_s I_s \sin \omega_s t}{\sqrt{1 - \left(\frac{I_o}{I_c} + \frac{I_s}{I_c} \cos \omega_s t\right)^2}}.$$

b. If $I_o \gg I_s$, show that the voltage can be approximated by

$$v = -\frac{\Phi_o}{2\pi I_c} \frac{\omega_s I_s \sin \omega_s t}{\sqrt{1 - \left(\frac{I_o}{I_c}\right)^2}}.$$

c. If $I_o \gg I_s$, show that the voltage can be described by a constant inductance L, which is given by

$$L = \frac{\Phi_o}{2\pi I_c \sqrt{1 - \left(\frac{I_o}{I_c}\right)^2}}.$$

d. In the opposite limit with $I_o \ll I_s$, show that the voltage can be approximated by

$$v = -\frac{\Phi_o}{2\pi I_c} \frac{\omega_s I_s \sin \omega_s t}{\sqrt{1 - \left(\frac{I_s}{I_c} \cos \omega_s t\right)^2}}.$$

e. Show that the dc component of the voltage is zero as long as $|I_o| + |I_s| < I_c$. Plot the current-voltage characteristic for the dc component of the voltage versus I_o .

Problem 8.5 (Voltage Impulse Response): Figure P8.2 shows a voltage source driving a single basic lumped Josephson junction that has a critical current of I_c . Let the junction initially have no currents or voltages across it.

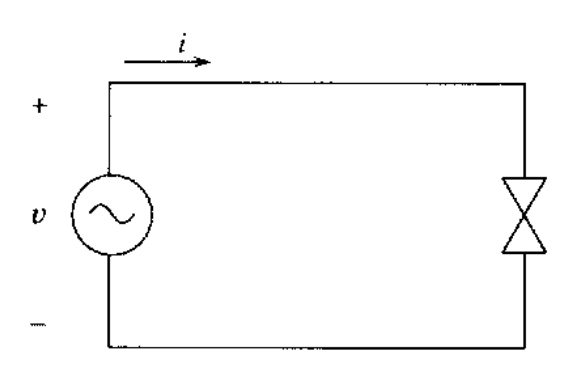


Figure P8.2 A Single Basic Lumped Junction Driven by a Voltage Source

a. Let an impulse of voltage be applied across the junction such that

$$v(t) = V'\delta(t),$$

where $\delta(t)$ is the unit impulse function (delta function). Show that the resulting impulse response of current is

$$i_{\text{imp}}(t) = I_c \sin\left(\frac{2\pi V'}{\Phi_o}\right) u(t),$$

where u(t) is the unit step function.

b. Suppose the voltage is a series of M impulses such that

$$v(t) = \sum_{n=1}^{M} V'_n \delta(t - t_n).$$

Show that the current is then

$$i(t) = I_c \sin \left(\frac{2\pi}{\Phi_o} \sum_{n=1}^M V'_n u(t-t_n) \right).$$

c. Explain why the response to a sum of voltage impulses is not the sum of the individual impulse responses.

Problem 8.6 (Current Step Response): A basic lumped junction is driven by a current source as in Figure P8.1. Also assume that there are no currents and voltages across the junction initially. Let the current be stepped across the junction such that

$$i(t) = I_o u(t),$$

where u(t) is the unit step function. Show that an impulse of voltage develops across the

junction such that

$$v(t) = \frac{\Phi_o}{2\pi} \sin^{-1} \left(\frac{I_o}{I_c}\right) \delta(t).$$

Explain how this is consistent with Problem 8.5.

Problem 8.7 (2D Josephson Junction): Consider the short junction in Figure 8.14. Let the applied magnetic flux density lie in a general direction in the y-z plane so that

$$\mathbf{B}_{\mathrm{app}} = \mathbf{B}_{o,y} \mathbf{i}_{y} + \mathbf{B}_{o,z} \mathbf{i}_{z}.$$

Generalize the argument in Section 8.5 to show that

$$i_{\max}(\Phi_J) = I_c \left| \frac{\sin \frac{\pi \Phi_{J,y}}{\Phi_o}}{\frac{\pi \Phi_{J,y}}{\Phi_o}} \right| \left| \frac{\sin \frac{\pi \Phi_{J,z}}{\Phi_o}}{\frac{\pi \Phi_{J,z}}{\Phi_o}} \right|,$$

where $\Phi_{J,y} = B_{o,y} h_{\text{eff}} w$ and $\Phi_{J,z} = B_{o,z} h_{\text{eff}} d$.

Problem 8.8 (2D Josephson Junction with Fourier Transform): Consider the short junction in Figure 8.14. As in Problem 8.7 let the applied magnetic flux density \mathbf{B}_{app} lie in a general direction in the y-z plane. Show that the maximum current can be written as the magnitude of the two dimensional Fourier transform of the current density

$$i_{\max} = \left| \int J_c(y,z) e^{j\mathbf{k}\cdot\mathbf{r}} da \right|,$$

where the integration is over all the 2D plane, \mathbf{r} is a position vector in the 2D y-z plane, and $d\mathbf{a}$ is the differential surface area in that plane. The Fourier transform vector is

$$\mathbf{k} = \frac{\Phi_o}{2\pi} \mathbf{B}_{\mathrm{app}} h_{\mathrm{eff}}.$$

Show that this gives the same result as Problem 8.7.

Problem 8.9 (Circular Josephson Junction): A Josephson junction with constant J_c is circular with a radius R. Use Problem 8.8 to show that no matter which direction the applied field B_o is in the plane of the junction,

$$i_{\max} = 2I_c \left| \frac{J_1(kR)}{kR} \right|,$$

where

$$I_c = J_c \pi R^2$$

and

$$k = \frac{\Phi_o}{2\pi} B_o h_{\rm eff} \,.$$

Here $J_1(x)$ is a first-order Bessel function of the first kind. Plot this result and compare it to that of a rectangular junction.

Problem 8.10 (Wave Equation for 2D Josephson Junction): Show that the wave equation for a long junction considered in Section 8.6, which has a constant critical current density J_c , generalizes to

$$\frac{\partial^2}{\partial y^2}\varphi(y,z) + \frac{\partial^2}{\partial z^2}\varphi(y,z) - \frac{1}{u_n^2}\frac{\partial^2}{\partial t^2}\varphi(y,z) = \frac{1}{\lambda_L^2}\sin\varphi(y,z).$$

Problem 8.11 (Effect of the Electrodes): The electrodes of the Josephson junction are now considered to be of arbitrary thicknesses b_1 and b_2 , as shown in Figure P8.3, and the penetration depths are λ_1 and λ_2 , respectively.

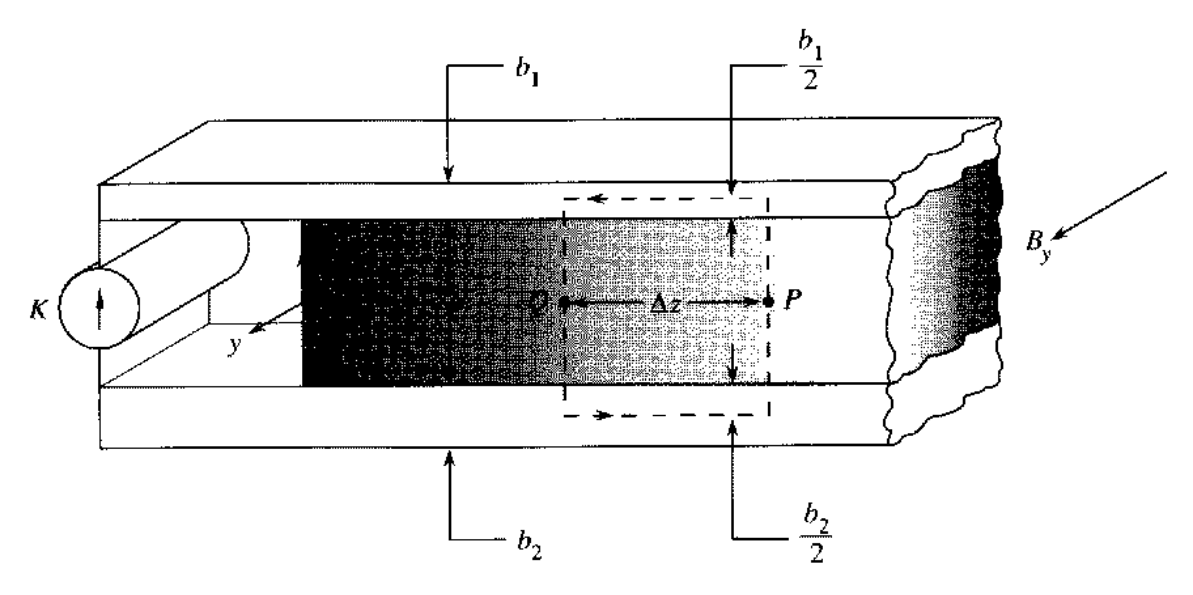


Figure P8.3 The cross section of a Josephson junction. The current flows across the junction in the *x*-direction.

a. Now consider two points Q and P, which are an infinitesimal distance Δz apart along the z-axis, which is taken to be in the center of the insulator. Take the contour of integration as shown in Figure P8.3. Show by an argument similar to that in Section 8.5 that

$$\varphi(P) - \varphi(Q) = \frac{2\pi\Phi}{\Phi_a} \,,$$

where Φ is the flux enclosed by the contour.

b. Show that for a short junction in an applied field B_o in the y-direction,

$$\Phi = B_o h_{\rm eff} \, \Delta z,$$

where the effective depth is given by

$$h_{ ext{eff}} = 2a + \lambda_1 anh rac{b_1}{2\lambda_1} + \lambda_2 anh rac{b_2}{2\lambda_2} \,.$$

c. Find h_{eff} in the limiting cases of the thicknesses being larger and smaller than the penetration depths.